

Advcanced Physics Lab SS19

# Experiment: SQUID

(Conducted on 23.09.19 with Jiwen Guan)

Erik Bode, Damian Lanzenstiel  
(Group 103)

October 2, 2019

## Abstract

The SQUID is used to measure magnetic fields very precisely. The SQUID itself is a superconductor ring with a Josephson contact. In this experiment the magnetic field of a conductor loop with different resistors should be measured. These were than compared to its theoretical value. The values are not comparable with each other. After this the magnetic fields of different test samples were measured. The measured data was plotted in polar representation depending on the angle of rotation.

# Contents

<b>1 Theoretical Background</b>	<b>2</b>
1.1 Superconductors . . . . .	2
1.2 BCS Theory . . . . .	2
1.3 Josephson effect . . . . .	2
1.4 Quantisation of magnetic flux . . . . .	3
1.5 The SQUID . . . . .	3
1.6 Lock-in Amplifier . . . . .	3
<b>2 Conduction of the experiment</b>	<b>4</b>
<b>3 Analysis</b>	<b>6</b>
3.1 The Conductor Loops . . . . .	6
3.2 Other Samples . . . . .	8
3.3 Polar Representation . . . . .	9
<b>4 Discussion</b>	<b>10</b>
<b>5 Tabeles</b>	<b>11</b>
<b>6 Figure</b>	<b>11</b>
<b>7 Bibliograpy</b>	<b>12</b>
<b>Literatur</b>	<b>12</b>
<b>8 Appendix</b>	<b>12</b>

# 1 Theoretical Background

Disclaimer: The theoretical information is, if not specified otherwise, taken from the manual [1] or the staatsexamen by V.Bange [2].

## 1.1 Superconductors

In general, superconductors are materials which, if cooled below a critical temperature  $T_c$ , show the following properties:

- The resistance of the material drops to an immeasurable level
- The material behaves like a almost perfect diamagnet: Magnetic fields induce a surface current, which compensates external magnetic fields completely (Meissner-Ochsenfeld effect)
- The electrons inside the material form Cooper pairs of two electrons bound together over a distance of hundreds of angstroms.

There are two types of superconductors:

- Low temperature superconductors:

The earliest discovered superconductors were of this type. The highest achievable critical Temperature is very low, usually requiring liquid helium cooling. E.g.  $Nb_3Ge$  with  $T_c = 23.2\text{ K}$ . Below a critical  $H_c$  field strength, magnetic fields do not penetrate the material beyond a few hundred nanometres.

- High temperature superconductors:

With this type, the critical temperature is higher. The highest temperature is  $T_C = 138\text{ K}$  with  $Hg_{12}Tl_3Ba_{30}Ca_{30}Cu_{45}O_{125}$ . This has the advantage that liquid nitrogen can be used as a coolant. There exist two critical magnetic field strengths,  $H_{c1}$  and  $H_{c2}$ . Below  $H_{c1}$ , the magnetic field is completely forced out of the material. Between both temperatures, magnetic flux-strings are forming inside the material which are normal conducting and enclosed by an eddy current.

## 1.2 BCS Theory

The BCS theory (Bardeen, Cooper, Schrieffer, 1957) explains many of the superconductor properties.

The lattice structure deforms in the orbit of an electron, since the nuclei needs a certain time, in the order of the inverse of the Debey frequency  $\omega_D(T \approx 10^{-13}\text{s})$ , to return to its initial location. This results in a weak positive polarization behind the considered electron, which attracts another electron over long distances, i.e. after an almost complete weakening of the repulsive Coulomb interaction. In theoretical solid state physics, the formation of a Cooper pair is described as follows: Electrons are fermions, i.e. each quantum mechanical state is occupied only once, except for two electrons with opposite spin. At low temperatures almost all states are now filled up to the Fermi energy  $E_F$ , above which the population density drops drastically towards 0. This results in a high probability of two electrons with antiparallel impulses to be found, which favours the formation of a Cooper pair. It is also said that even relatively weak interactions lead to bound states. These combined spin 1/2 systems then have total spin 0 and behave like bosons. According to the Bose statistics, any number of bosons can occupy a state, so there is no limit for the creation of Cooper pairs. And the material is now in a superconducting state. The bosonic behaviour of the Cooper pairs causes the formation of a total wave function which is present in the ground state. This total wave has some consequences, like the flux quantization, resistance-free charge transport and effects at a Josephson contact. The wavelength of the bosonic wave functions is very large compared to the distances of the atomic bodies in the lattice, since the interaction between the electrons is very weak. Therefore, these or lattice oscillations are not obstacles for the Cooper pairs. Thus a resistance-free charge transport is given.

## 1.3 Josephson effect

The Josephson effect is the underlying principle of a Josephson junction, a core part of the SQUID sensor. The quantum mechanical phenomenon of tunnelling also occurs between two superconductors separated by a thin insulating layer. The insulation layer must not be a superconductor. This is essential for the SQUID experiment, since a magnetic field applied from the outside cannot penetrate into the

superconductor (Meissner-Ochsenfeld effect), but into the insulating layer. The Cooper pairs can now tunnel into the other superconductors if phase difference  $\Delta\phi = n \cdot \pi$ . A current flows, without a potential difference. Also the pairs lose no energy while tunnelling, i.e. classically regarded there is no resistance. This seems paradoxical compared to the classical Ohm's law  $U = R \cdot I$ . Since the insulating layer is not a superconductor, magnetic fields can penetrate it. This influences the correlation of the wave functions of the tunnelling Cooper pairs, i.e. the phase difference  $\Delta\phi$ , which is a measurable change of the current. The tunnel current through the barrier is given by:

$$I_S = I_C \sin(\Delta\phi)$$

## 1.4 Quantisation of magnetic flux

The magnetic flux in the circular superconductor is quantised as

$$\oint \vec{A} d\vec{l} = \Phi_B \text{ for } \nabla \times \vec{A} = \vec{B}$$

where  $\Phi_B$  is the magnetic flux inside the superconducting ring. Because all the Cooper pairs are in the BSC ground state, their wave functions have definite phase relations. This is the reason of the quantization of the magnetic flux in levels of the magnetic flux quantum  $\Phi_0$  as in

$$|\Phi_B| = n \frac{\hbar}{2e} = n\Phi_0$$

## 1.5 The SQUID

The SQUID (Superconducting QUantum Interference Device) is a very precise sensor to detect changes in magnetic fields in the order of the flux quantum. The one used during the experiment is a RF SQUID, which has one Josephson junction inside the superconducting ring. A RF circuit generates an external magnetic flux  $\Phi_{ext}$ . This flux induces a current in the superconducting ring to compensate the external field that  $\Phi_{int}$  is zero. Since the total wave function of the Cooper pairs carrying the current must be constant inside the superconductor, the total flux  $\Phi_{tot}$  can only be changed as multiples of the flux quantum. The Josephson contact shifts the phase of the total wave function. The phase difference can be calculated as:

$$\theta_2 - \theta_1 = 2\pi n - 2\pi \frac{\Phi_{tot}}{\Phi_0}$$

A change of the external flux can not change the flux inside the superconducting ring, if the difference is smaller than  $\Phi_0$ . These differences are compensated by a surface current which results in a surface flux  $\Phi_S = LI_S$  that  $\Phi_{tot} = \Phi_{ext} - \Phi_S$ . The inductance  $L$  is dependant on the shape and material. If the change of flux is bigger than  $\Phi_0$ , the superconductivity is interrupted while  $\Phi_{int}$  is increasing. When the superconducting state is established again, the remaining flux difference smaller than  $\Phi_0$  is compensated as above.

For superconductors with a Josephson junction this is also true, although here the external magnetic field necessitates the flux quantization inside the superconductor. This results in a more complex behaviour, when  $I_S = I_{S,max} \sin(\theta_2 - \theta_1)$ :

$$\Phi_{tot} = \Phi_{ext} + LI_{S,max} \sin\left(2\pi \frac{\Phi_{tot}}{\Phi_0}\right)$$

## 1.6 Lock-in Amplifier

A lock-in amplifier compares a data signal with a reference signal. It only amplifies the part of the data signal, which has the same frequency and is in phase with the reference signal. It is especially useful for signals with a low signal to noise ratio.

## 2 Conduction of the experiment

After the entrance exam the distances on the lid of the Dewar with the SQUID probe and the distance between the top of the Dewar and the position of the sample to later be able to compute the distance between the sample and the sensor. All distances were measured three times to reduce the measurement inaccuracy. After that was finished, the Dewar was filled with the liquid nitrogen and the SQUID probe was placed inside to cool it down. While the sensor is cooling, the loop of the resistor measurements was measured from different angles because it is quite asymmetric.

Now, after approx. 15 minutes, the VCA and VCO settings in the control software of the SQUID were set as a calibration. They were modified so the SQUID signal has, as seen in figure 1, the characteristic differences from the usual sine function at the maxima and minima of the triangular reference voltage are as visible as possible.

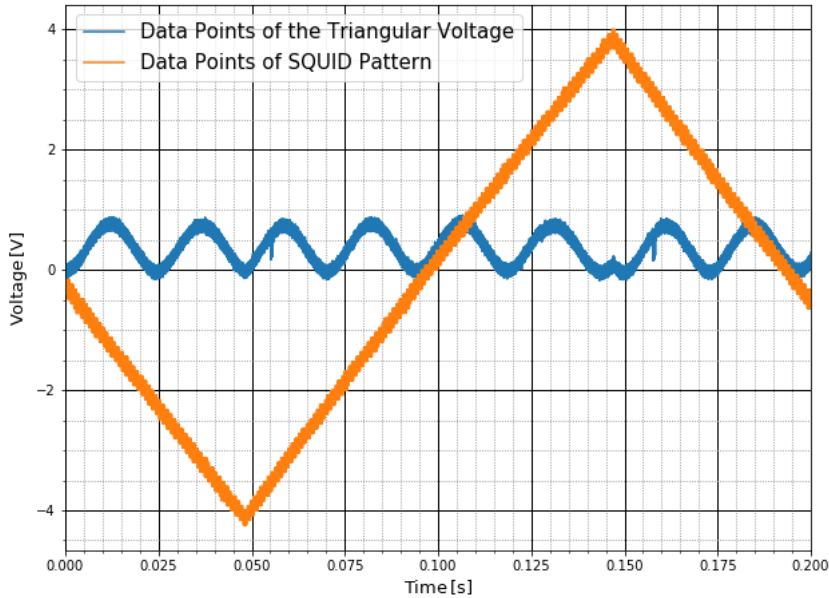


Figure 1: The figure shows the SQUID signal after being calibrated for the measurement.

Now, after measuring the battery voltages, the measurements for the resistors were conducted. Starting with the smallest, four measurements of every resistor for each used motor speed were made. For the first resistor, the speed settings 10, 5 and 2 were used. During the measurements of the second resistor, it became clear that measurements of with the speed of 2 are not viable due to an increase in background interference. For the other resistors, only the speeds 10 and 5 were used and, also due to the increased background instabilities, only three measurements each were made. After finishing the resistor measurements, the rotational speed of the motor settings 10 and 5 was measured over multiple rotations.

Now five different other samples were measured, each at a speed set to 10. The samples can be seen in figure 2 First a iron splinter, which worked well. Second a gold plate was tried, which did unfortunately not seem to have any measurable dipole moment. After taking two measurements, the signal suddenly disappeared and it seemed like, nothing was inside of the SQUID apparatus. Because there was a signal, the measurement should be retried later. The third sample was a magnet splinter, which also worked well. After that, the gold sample was retried, and still no signal was measurable. Now, a stone was measured. After this, the gold sample was retried one last time, but it still showed no signal at all. As a last sample, a magnet was measured. It was chosen as the last sample, because it influences the detector so strong that for the rest of the day no other measurements can be made.

As the last measurement, the resistors were measured with the multimeter.

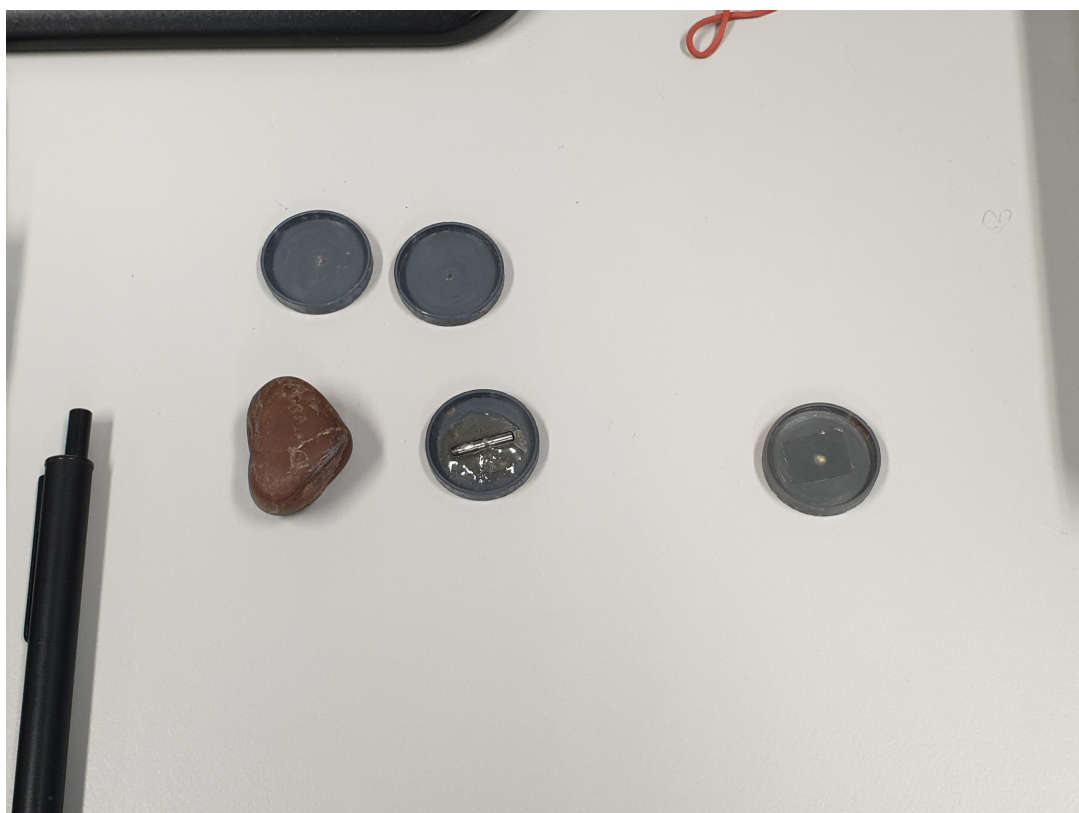


Figure 2: The picture shows the other five samples used during the experiment. In the quadratic arranged samples, the top right one is the iron splinter, the top left is the magnet splinter. The bottom left one is the stone, the bottom right one is the magnet. To the right of the other samples, the gold sample is placed.

### 3 Analysis

#### 3.1 The Conductor Loops

To calculate the  $B_z$  value and the dipole moment  $p$ , there are two different way. The first one is to calculate the theoretical magnetic field as well as dipole moment by using the properties of the conductor loop and the applied voltage.

Here the equation 1 was used.

$$p(R) = AI(R) = \pi r^2 I(R) = \pi r^2 \frac{U}{R} \quad (1)$$

The error is than computed using Gaussian error propagation by following equation:

$$\sigma_p = \sqrt{\left(\frac{\pi Ur\sigma_r}{R}\right)^2 + \left(\frac{\pi r^2\sigma_U}{R}\right)^2 + \left(\frac{\pi r^2U\sigma_R}{R^2}\right)^2} \quad (2)$$

The diameter  $d$  of the loop was measured multiples times and the mean was taken to get the radius . The error of the mean was calculated using equation 3. After this the value was divided by 2 to get the radius.

$$\sigma_x = \sqrt{\left(\frac{1}{n-1} \sum_{i=1}^n (x_i - \bar{x})^2\right)} \quad (3)$$

The voltage was gained by measuring the two attached batteries and adding them together. The values for the different resistors were given in the manual of the experiment[1] and are noted in table 1.

$$r = (1.558 \pm 0.010) \text{ mm}$$

$$U_{ges} = U_1 + U_2 = (1.459 \pm 0.005 + 1.494 \pm 0.005) \text{ V} = (2.9530 \pm 0.0007) \text{ V}$$

With this the dipole moment for the different Resistors was calculated and are written down in table 2.

	Resistor 1	Resistor 2	Resistor 3	Resistor 4	Resistor 5
$\Omega$	$51.47 \pm 0.05$	$100.80 \pm 0.10$	$300.80 \pm 0.30$	$510.6 \pm 0.5$	$1000.0 \pm 1.0$

Table 1: Different Resistors for the five conductor loop measurements.

It can now be used to compute the magnetic field  $B_z$  using equation 4.

$$B_z = \frac{\mu_0 p}{2\pi z^3} \quad (4)$$

In this equation the value  $z$  is the distance of the probe to the SQUID. This was measured by measuring the length of the kryostat from top to the probe as well as from the top to the SQUID. The difference of both is the distance from probe to SQUID. To decrease the errors the mean of multiple distance measurements were taken.

$$z = (2.65 \pm 0.12) \text{ cm}$$

The with that calculated value  $B_z$  is also in table 2.

	$p [\text{Am}^2]$	$B_z [\text{T}]$
R1	$(8.75 \pm 0.11) \times 10^{-7}$	$(9.4 \pm 1.2) \times 10^{-9}$
R2	$(4.47 \pm 0.06) \times 10^{-7}$	$(4.8 \pm 0.6) \times 10^{-9}$
R3	$(1.498 \pm 0.020) \times 10^{-7}$	$(1.61 \pm 0.21) \times 10^{-9}$
R4	$(8.82 \pm 0.12) \times 10^{-8}$	$(9.5 \pm 1.2) \times 10^{-10}$
R5	$(4.51 \pm 0.06) \times 10^{-8}$	$(4.8 \pm 0.6) \times 10^{-10}$

Table 2: Values of the magnetic field and the dipole moment for the five different resistors. Calculated by using equation 1 and 4

The other way to calculate the dipole moment and magnetic field was by using the measured signals of the SQUID. Here the signal shapes were fitted with the help of Python's package `scipy.optimize`[3] with the method `curve_fit`. Here the form given in equation 5 was used. With that the offset  $a$ , the frequency  $\omega = c$  as well as the amplitude  $b = \Delta V$  can be calculated.

$$f(x) = a + b \sin(cx + d) \quad (5)$$

An example of the fits can be seen in figure 3 the other ones are in the appendix.

The parameters  $b$  of the different measurements for each resistor were taken and the weighted mean of them was taken. For this mean the equation 6 and 7 were used. The values are listed in table 3.

$$\bar{x}_g = \frac{\sum_i g_i x_i}{\sum_i g_i} \quad \text{with} \quad g_i = \frac{1}{\sigma_i^2} \quad (6)$$

$$\sigma_{\bar{x}_g} = \frac{1}{\sqrt{\sum_i 1/\sigma_i^2}} \quad (7)$$

With these voltages the magnetic field  $B_z$  can be computed using equation 8. An similar to the calculation for the theoretical values equation 4 can be used to gain the dipole moment  $p$ .

$$B_z = F \frac{\Delta V}{s_i} \quad (8)$$

The value of  $F$  the field flux coefficient is  $9.3 \frac{nT}{\Phi_0}$  and  $s_i$  is transfer coefficient. This one can be looked up in the manual[1]. For the conductor loops a FB-R resistance of  $100 \text{ k}\Omega$  was chosen which leads to a  $s_i$  value of  $1900 \frac{mV}{\Phi_0}$ . The values of the calculated magnetic field and dipole moment are noted in table 3

	$p[\text{Am}^2]$	$B_z[\text{T}]$	$\Delta V[\text{V}]$
R1	$(2.19 \pm 0.29) \times 10^{-7}$	$(2.356 \pm 0.007) \times 10^{-9}$	$0.2407 \pm 0.0007$
R2	$(1.18 \pm 0.15) \times 10^{-7}$	$(1.271 \pm 0.007) \times 10^{-9}$	$0.1298 \pm 0.0007$
R3	$(3.9 \pm 0.5) \times 10^{-8}$	$(4.17 \pm 0.08) \times 10^{-10}$	$0.0426 \pm 0.0008$
R4	$(2.36 \pm 0.31) \times 10^{-8}$	$(2.54 \pm 0.05) \times 10^{-10}$	$0.0259 \pm 0.0005$
R5	$(1.37 \pm 0.19) \times 10^{-8}$	$(1.47 \pm 0.06) \times 10^{-10}$	$0.0150 \pm 0.0006$

Table 3: Measured values for the different conductor loops using the fits of the SQUID signals.

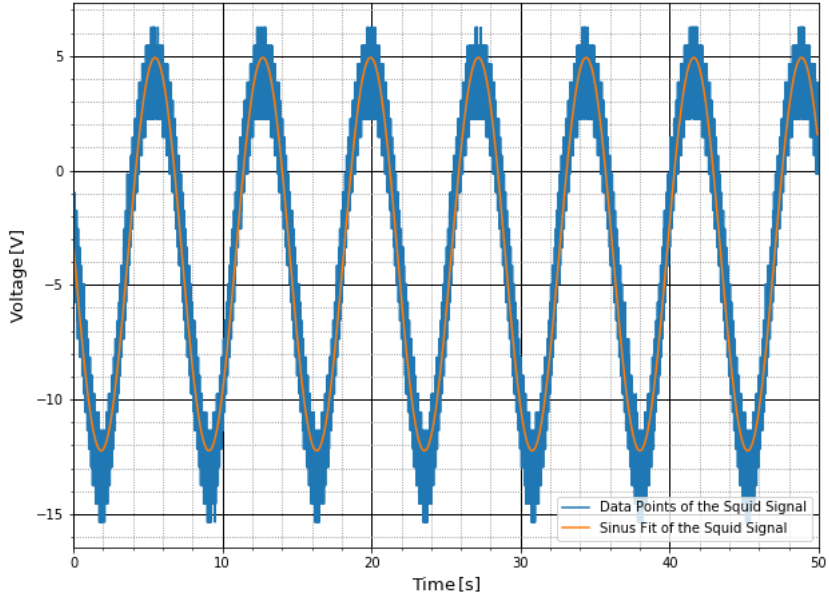


Figure 3: In blue the signal coming from the SQUID and in orange the sinus fit to the data points.

### 3.2 Other Samples

During the measurement other samples were tested with the SQUID. The SQUID signals were analysed in a similar way to the conductor Loops before. The sinus of the form 5 was fitted on the signal. The mean of amplitude which is parameter  $b$  was computed for the different samples and with this the magnetic field  $B_z$  and dipole moment could be calculated and can be found in table 4 in the table below. It is also important to note that for the calculation of the Magnet another value for  $s_i$  had to be used since the FB-R value was changed to  $1\text{ k}\Omega$ . The here used value for  $s_i$  was  $21 \frac{\text{mV}}{\Phi_0}$

	$p[\text{Am}^2]$	$B_z[\text{T}]$	$\Delta V [\text{V}]$
Iron chips	$(1.84 \pm 0.25) \times 10^{-8}$	$(1.98 \pm 0.07) \times 10^{-10}$	$0.0202 \pm 0.0007$
Gold lamella	$(3.2 \pm 0.4) \times 10^{-8}$	$(3.42 \pm 0.12) \times 10^{-10}$	$0.0349 \pm 0.0012$
Magnet chips	$(7.8 \pm 1.0) \times 10^{-6}$	$(8.408 \pm 0.030) \times 10^{-8}$	$8.589 \pm 0.031$
Stone	$(7.4 \pm 1.1) \times 10^{-10}$	$(7.9 \pm 0.5) \times 10^{-12}$	$0.00081 \pm 0.00005$
Magnet	$0.000262 \pm 0.000034$	$(2.814 \pm 0.014) \times 10^{-6}$	$6.355 \pm 0.031$

Table 4: Measured and calculated values for different materials and forms of samples.

### 3.3 Polar Representation

For the samples and conductor loops the polar representation should be plotted. For this one period of the data points was taken. With the help of the coordinate transformation of the manual[1]:

$$x_i = |B_z| \cdot \cos(\alpha) \quad (9)$$

$$y_i = |B_z| \cdot \sin(\alpha) \quad (10)$$

The values for  $\alpha$  and  $B_z$  are computed using the measured values for time and voltage of the data point as well as the parameter of the fits.

$$\alpha_i = c_i t_i + d_i \quad |U_i - a_i| \cdot \frac{F}{s_i} \quad (11)$$

For the stone the polar representation can be seen in figure 4, the rest is in the appendix.

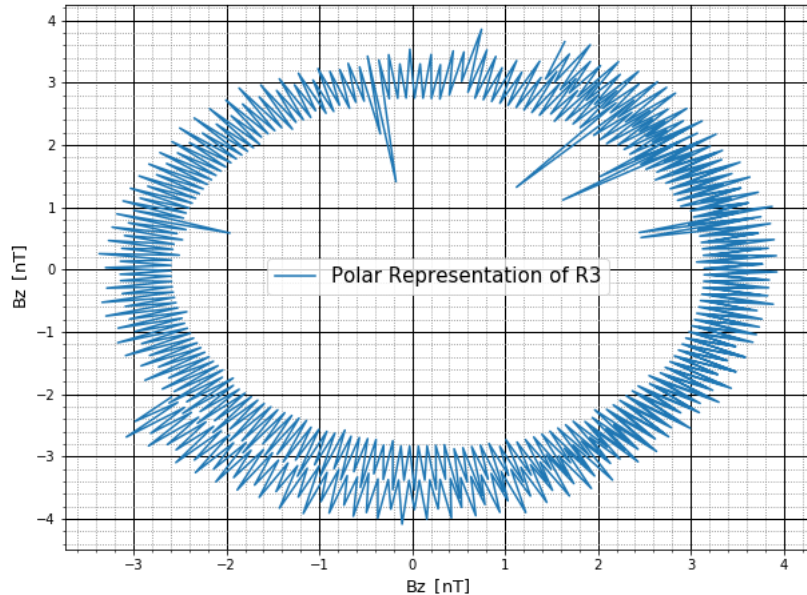


Figure 4: Polar Representation for one period of the signal coming from the R2 Conductor Loop.

## 4 Discussion

In the experiment the magnetic field and dipole moment of loops with different resistors had to be calculated with the help of data measured by the SQUID (see table 3). This can be compared to the theoretical value of the loops which can be seen in table 2. The strength of the magnetic field  $B_z$  is compared with equation 12:

$$t = \frac{|x_1 - x_2|}{\sqrt{\sigma_x 1^2 + \sigma_x 2^2}} \quad (12)$$

As can be seen in the table 5 the values aren't compatible with each other. Looking at the values we

	R1	R2	R3	R4	R5
t[ $\sigma$ ]	5.705	5.598	5.635	5.570	5.276

Table 5: Comparison of the magnetic field values  $B_z$  with equation 12

see that they are different by a factor of 4. The reason for this big difference probably due to a larger than expected error by the measurement of the distance between probe and SQUID sensor. Here the measurement wasn't very precise due to the lack of a good way to measure it. The impact on the results is also increased to its huge influence due to the fact that the magnetic field is proportional to  $\frac{1}{z^3}$  (see eq:8). That means that even small differences can make a huge difference in the results. Another reason for errors is the form of the loop. It wasn't very symmetrical to begin with which makes  $A = \pi r^2$  in the equation 1 only a rough estimation. The measurement with the SQUID is naturally also not perfect due to the huge amount of outer magnetic field which influence the measurement. It was especially hard to measure the weaker magnetic fields since the background noise was even with the Lock-In filter quite high.

In the second part of the experiment different samples were measured. Here the problem of the noise can be seen very good at the sample of a stone see figure: 49. Here the signal is mostly hidden in noise so the fit is very also not very accurate. Also there is no value to compare these samples to we still see some expected values. For example is the B-field of the magnet very big compared to the other samples. The magnetic chips are also not to low compared to the others. The stone on the other side has the lowest field. If we compare the polar representations with the ones of the loop its also noticeable, that the samples aren't as symmetrical any more.

## 5 Tabeles

### List of Tables

1	Resistors . . . . .	6
2	Values of Dipole Moment and Magnetic Field . . . . .	6
3	Values of the Loops with the Fit Method . . . . .	7
4	Values of the Samples with the Fit Method . . . . .	8
5	Vergleich der Magnetfelder . . . . .	10

## 6 Figure

### List of Figures

1	Picture of the calibration of the SQUID . . . . .	4
2	Picture of the other samples . . . . .	5
3	Example of the Data Plots with SINus Fit . . . . .	8
4	Polar Representation for R2 Conductor Loop . . . . .	9
5	Plot of first conductor loop 1 . . . . .	13
6	Plot of first conductor loop 2 . . . . .	14
7	Plot of first conductor loop 3 . . . . .	14
8	Plot of first conductor loop 4 . . . . .	15
9	Plot of first conductor loop 5 . . . . .	15
10	Plot of first conductor loop 6 . . . . .	16
11	Plot of first conductor loop 7 . . . . .	16
12	Plot of first conductor loop 8 . . . . .	17
13	Polar Representation for R1 Conductor Loop . . . . .	17
14	Plot of second conductor loop 1 . . . . .	18
15	Plot of second conductor loop 2 . . . . .	18
16	Plot of second conductor loop 3 . . . . .	19
17	Plot of second conductor loop 4 . . . . .	19
18	Plot of second conductor loop 5 . . . . .	20
19	Plot of second conductor loop 6 . . . . .	20
20	Plot of second conductor loop 7 . . . . .	21
21	Plot of third conductor loop 1 . . . . .	21
22	Polar Representation for R3 Conductor Loop . . . . .	22
23	Plot of fourth conductor loop 1 . . . . .	22
24	Plot of fourth conductor loop 2 . . . . .	23
25	Plot of fourth conductor loop 3 . . . . .	23
26	Plot of fourth conductor loop 4 . . . . .	24
27	Plot of fourth conductor loop 5 . . . . .	24
28	Polar Representation for R4 Conductor Loop . . . . .	25
29	Plot of fifth conductor loop 1 . . . . .	25
30	Plot of fifth conductor loop 2 . . . . .	26
31	Plot of fifth conductor loop 3 . . . . .	26
32	Polar Representation for R5 Conductor Loop . . . . .	27
33	SQUID signal of Iron Chips 1 . . . . .	27
34	SQUID signal of Iron Chips 2 . . . . .	28
35	SQUID signal of Iron Chips 3 . . . . .	28
36	SQUID signal of Iron Chips 4 . . . . .	29
37	Polar Representation for Iron Chips . . . . .	29
38	SQUID signal of a Gold Slide 1 . . . . .	30
39	SQUID signal of a Gold Slide 2 . . . . .	30
40	Polar Representation for Gold Slide . . . . .	31
41	SQUID signal of Magnet Chips 1 . . . . .	31
42	SQUID signal of Magnet Chips 2 . . . . .	32
43	SQUID signal of Magnet Chips 3 . . . . .	32

44	SQUID signal of Magnet Chips 4 . . . . .	33
45	Polar Representation for Magnet Chips . . . . .	33
46	SQUID signal of a Stone 1 . . . . .	34
47	SQUID signal of a Stone 2 . . . . .	34
48	SQUID signal of a Stone 3 . . . . .	35
49	SQUID signal of Stone 4 . . . . .	35
50	Polar Representation for a Stone . . . . .	36
51	SQUID signal of a Magnet 1 . . . . .	36
52	SQUID signal of a Magnet 2 . . . . .	37
53	Polar Representation for a Magnet . . . . .	37

## 7 Bibliography

### References

- [1] *Versuchsanleitung: Fortgeschrittenen Praktikum Teil 1 Kernspin.*
- [2] Volker Bange. Einrichtung des versuches "squid", 2000.
- [3] Eric Jones, Travis Oliphant, Pearu Peterson, et al. Python3 package `scipy.optimize` for curve fitting., 2001–.

## 8 Appendix

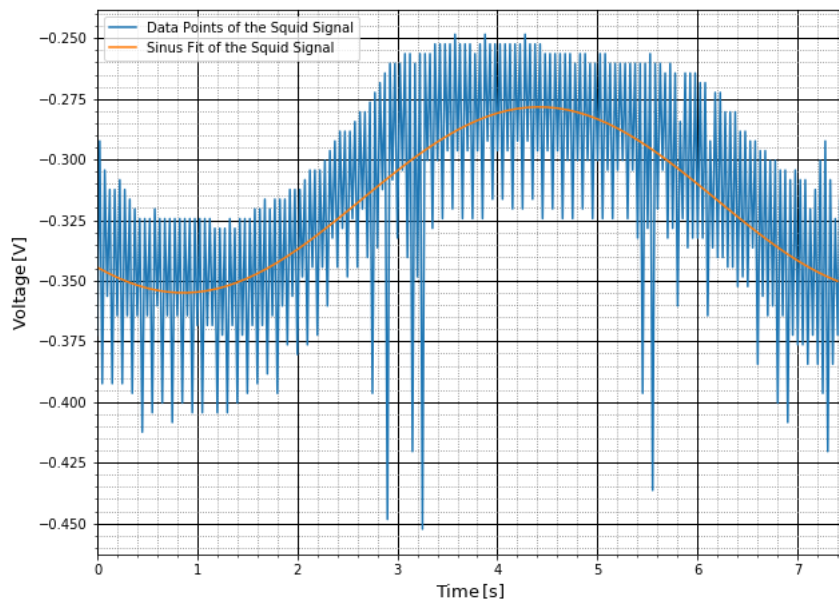


Figure 5: Plot 1 of the first conductor loop with resistor R1. The speed of the rotation here was 5. In orange is the sinus fit of the data point.

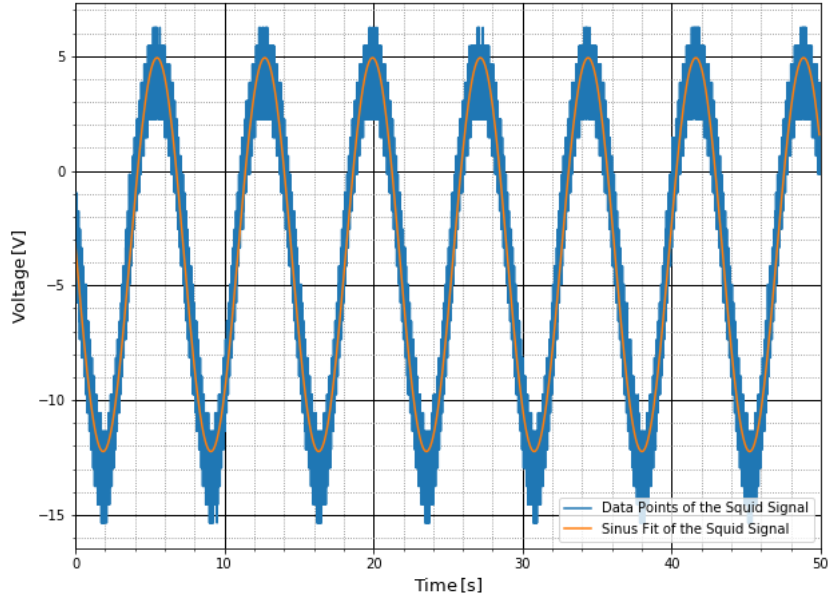


Figure 6: Plot 2 of the first conductor loop with resistor R1. The speed of the rotation here was 5. In orange is the sinus fit of the data point.

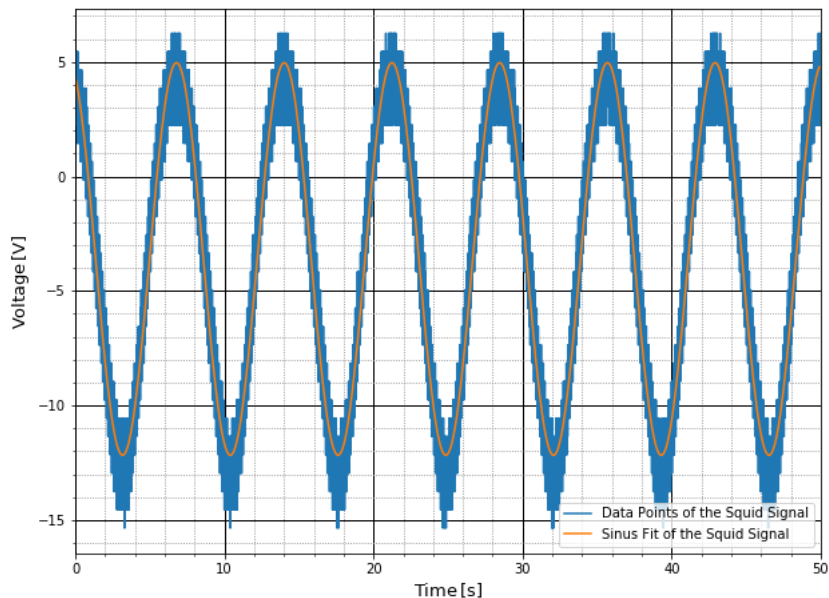


Figure 7: Plot 3 of the first conductor loop with resistor R1. The speed of the rotation here was 5. In orange is the sinus fit of the data point.

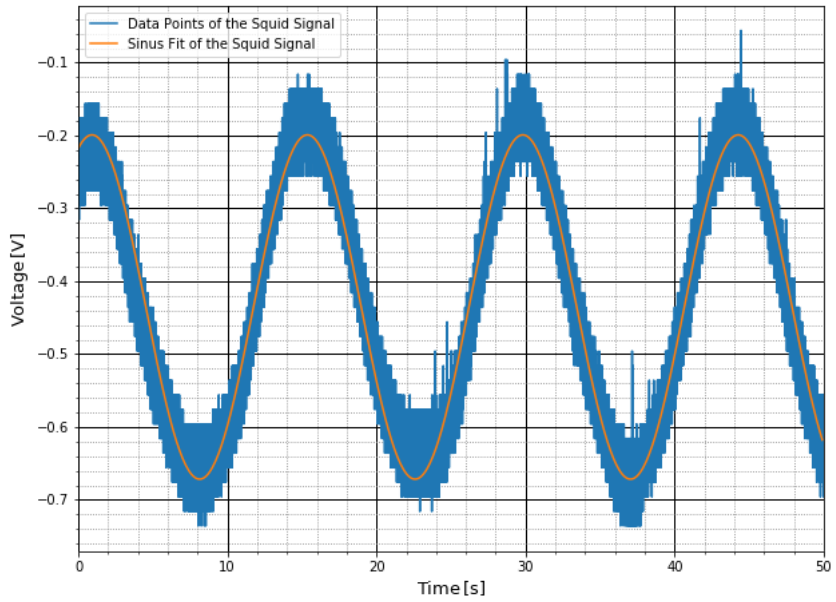


Figure 8: Plot 4 of the first conductor loop with resistor R1. The speed of the rotation here was 5. In orange is the sinus fit of the data point.

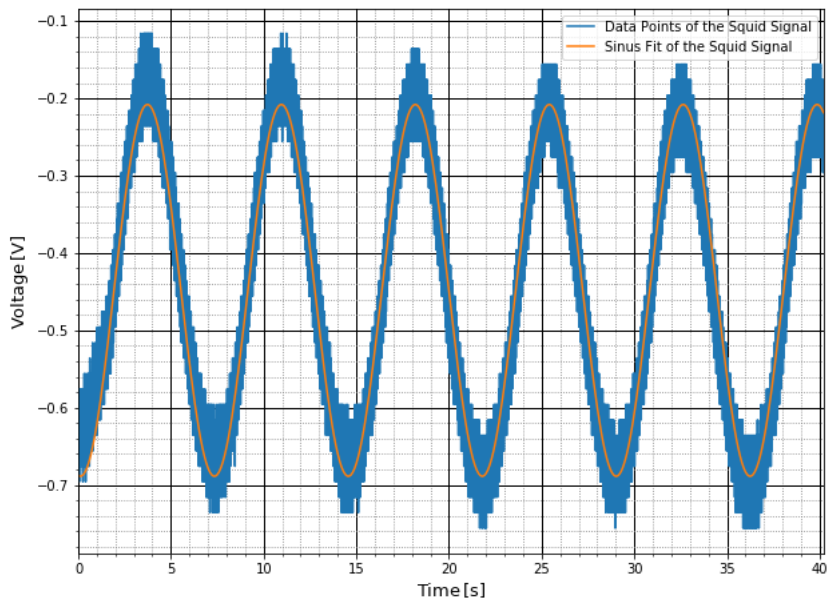


Figure 9: Plot 5 of the first conductor loop with resistor R1. The speed of the rotation here was 10. In orange is the sinus fit of the data point.

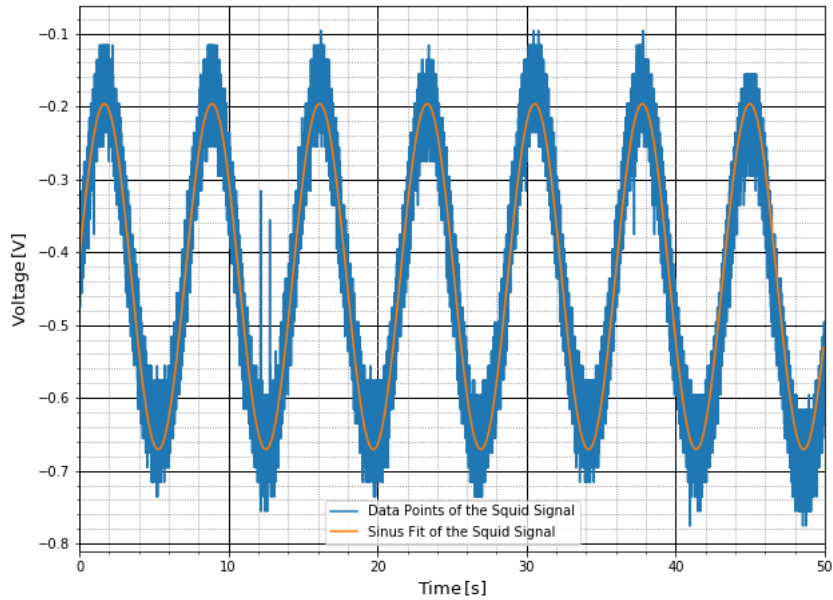


Figure 10: Plot 6 of the first conductor loop with resistor R1. The speed of the rotation here was 10. In orange is the sinus fit of the data point.

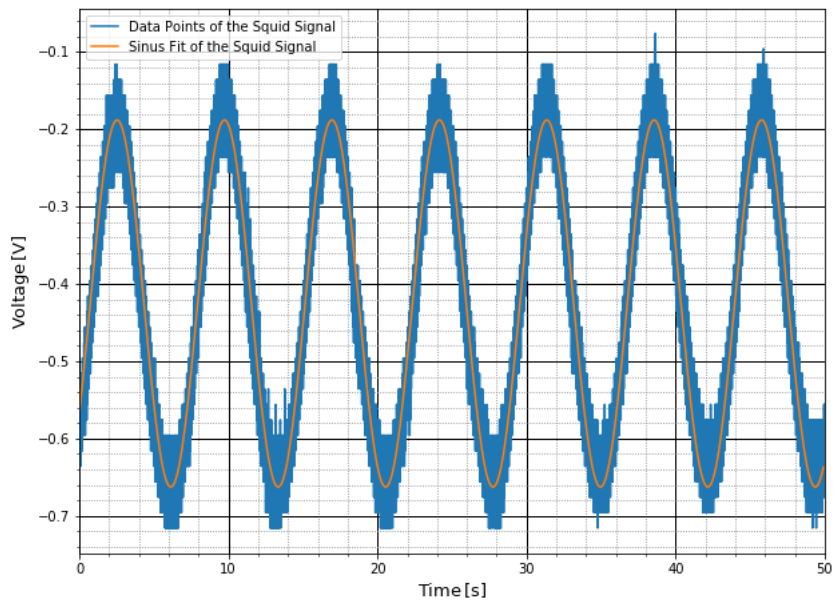


Figure 11: Plot 7 of the first conductor loop with resistor R1. The speed of the rotation here was 10. In orange is the sinus fit of the data point.

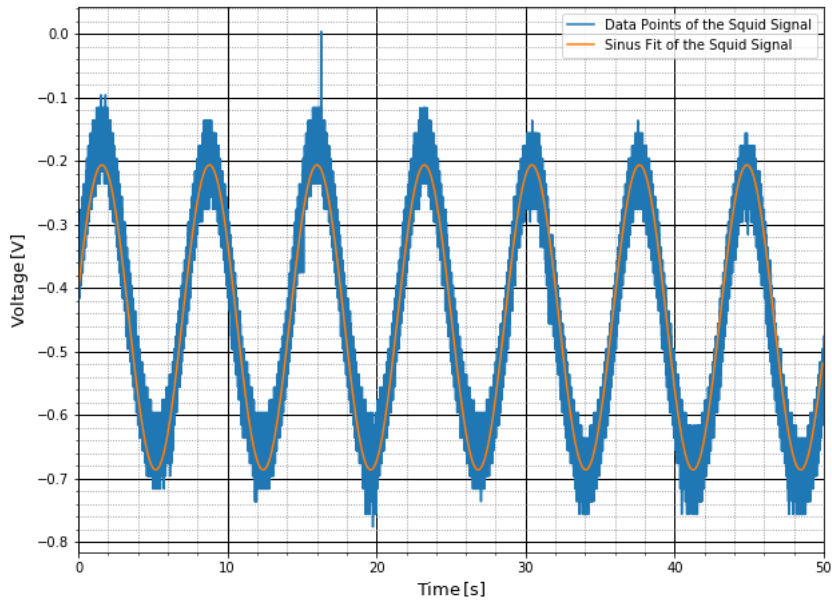


Figure 12: Plot 8 of the first conductor loop with resistor R1. The speed of the rotation here was 10. In orange is the sinus fit of the data point.

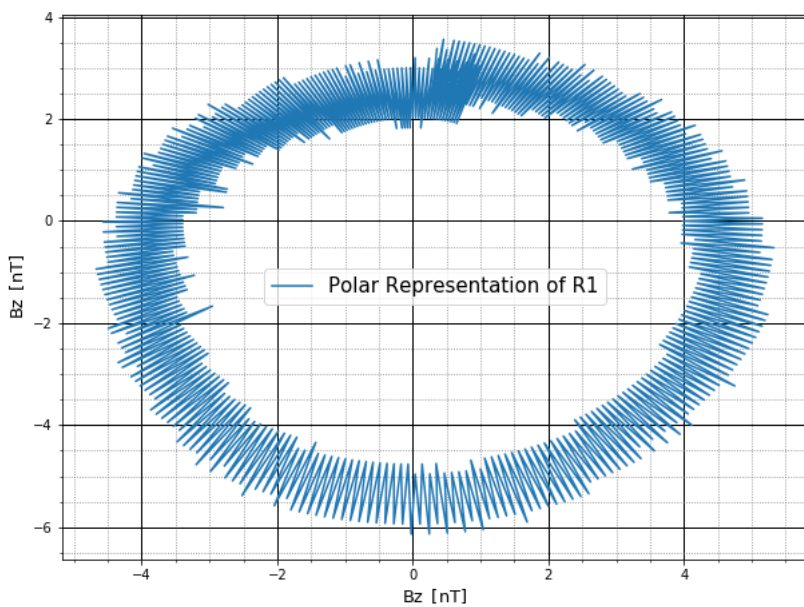


Figure 13: Polar Representation for one period of the signal coming from the R1 Conductor Loop.

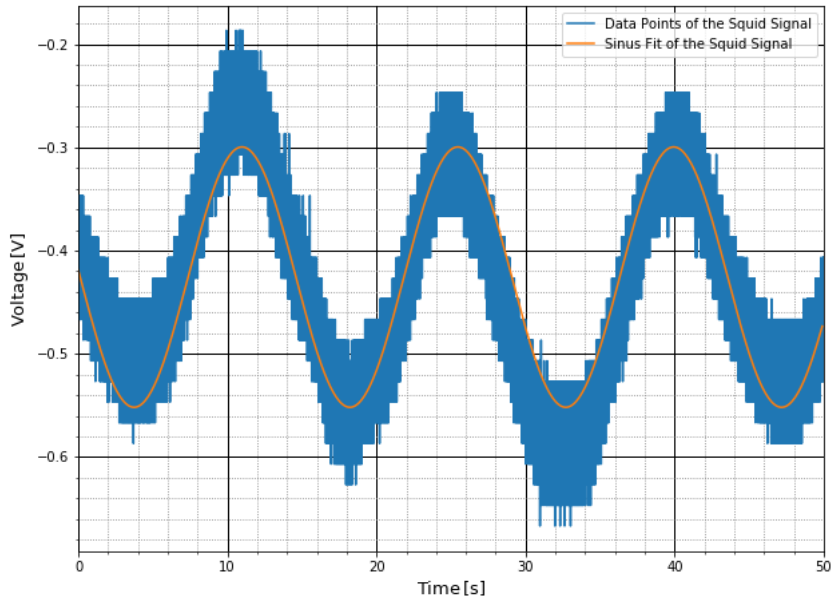


Figure 14: Plot 1 of the second conductor loop with resistor 2. The speed of the rotation here was 5. In orange is the sinus fit of the data point.

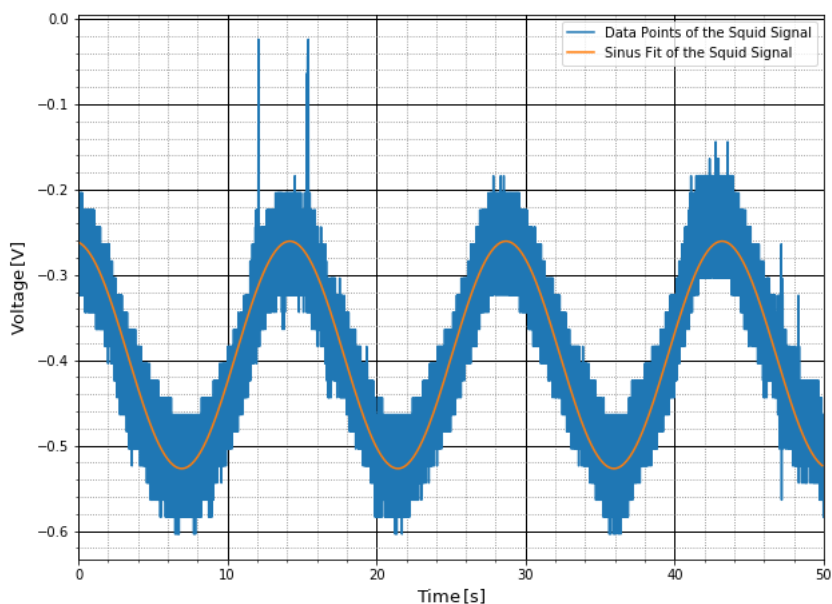


Figure 15: Plot 2 of the second conductor loop with resistor 2. The speed of the rotation here was 5. In orange is the sinus fit of the data point.

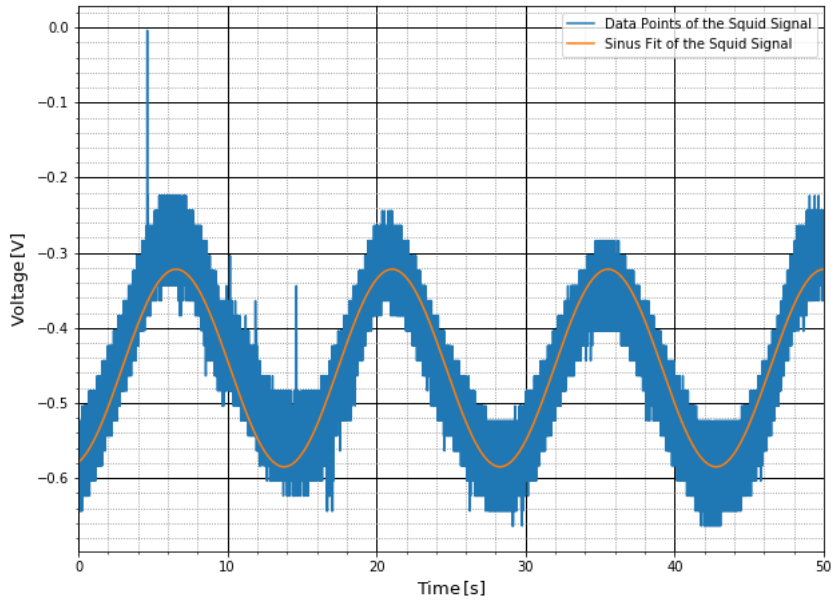


Figure 16: Plot 3 of the second conductor loop with resistor 2. The speed of the rotation here was 5. In orange is the sinus fit of the data point.

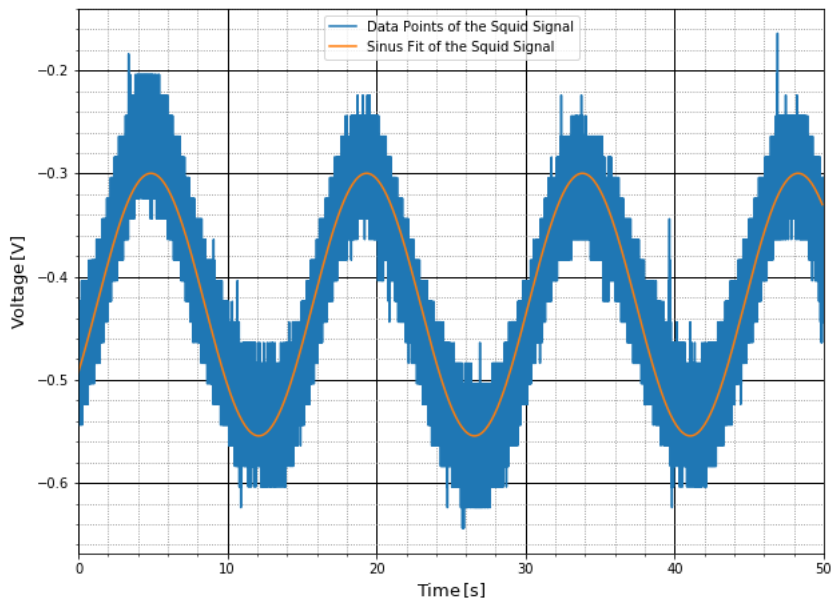


Figure 17: Plot 4 of the second conductor loop with resistor 2. The speed of the rotation here was 5. In orange is the sinus fit of the data point.

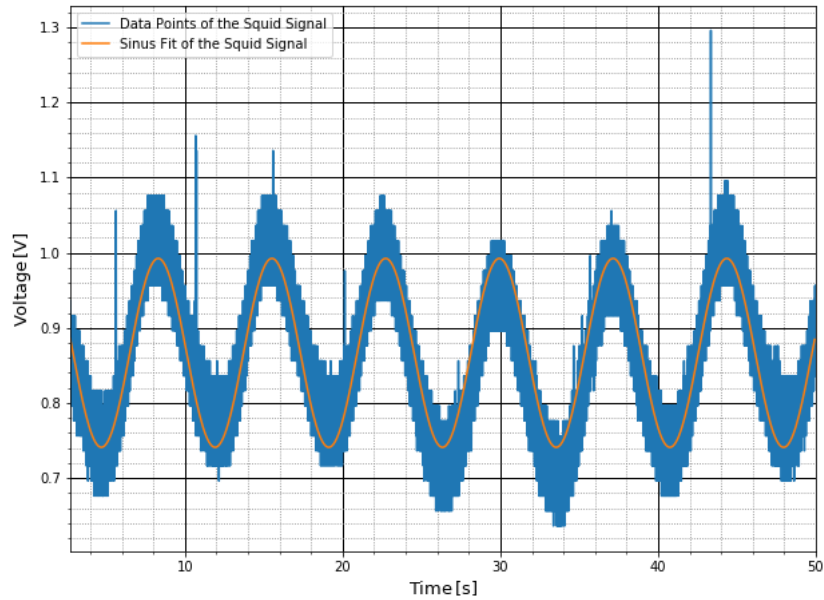


Figure 18: Plot 5 of the second conductor loop with resistor 2. The speed of the rotation here was 10. In orange is the sinus fit of the data point.

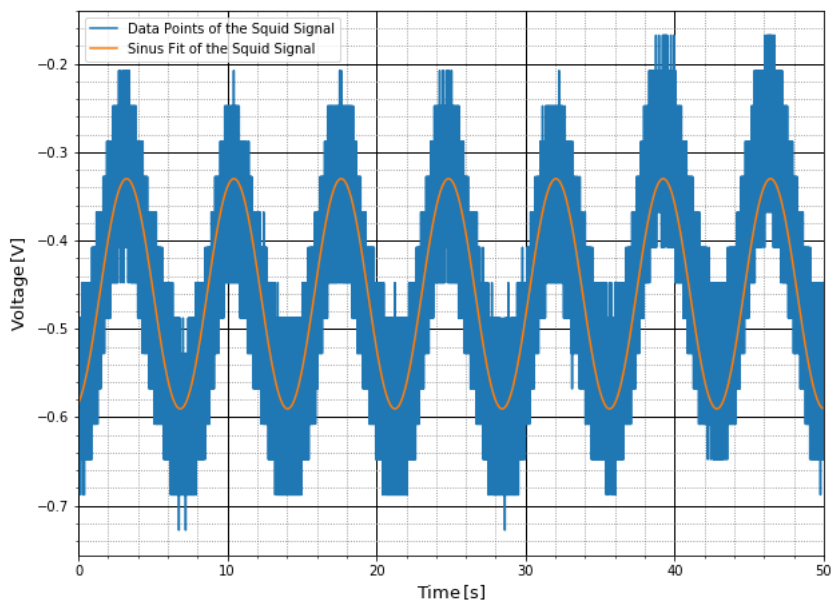


Figure 19: Plot 6 of the second conductor loop with resistor 2. The speed of the rotation here was 10. In orange is the sinus fit of the data point.

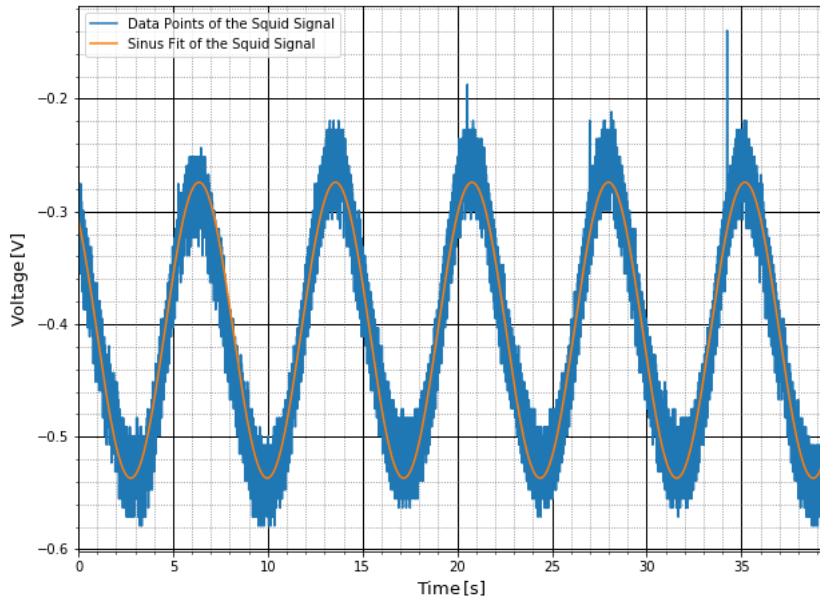


Figure 20: Plot 7 of the second conductor loop with resistor 2. The speed of the rotation here was 10. In orange is the sinus fit of the data point.

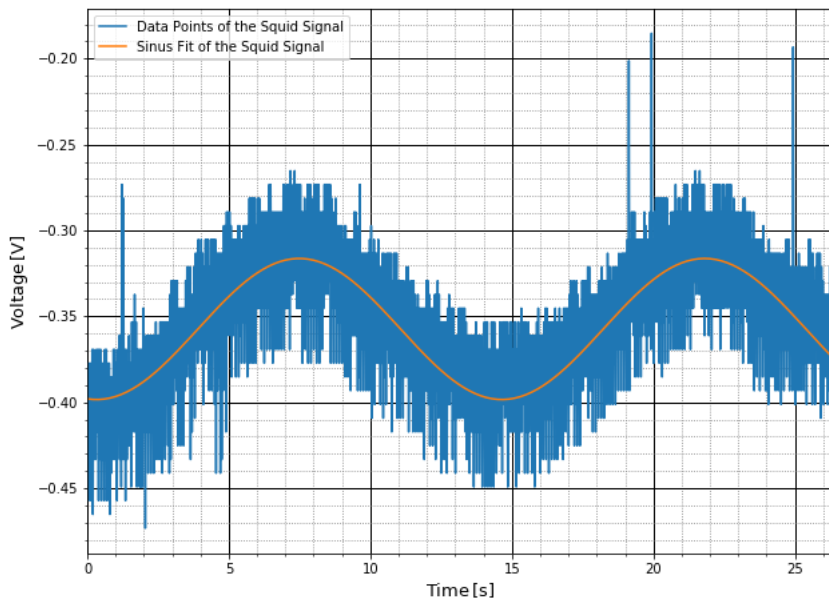


Figure 21: Plot 1 of the third conductor loop with resistor 3. The speed of the rotation here was 5. In orange is the sinus fit of the data point.

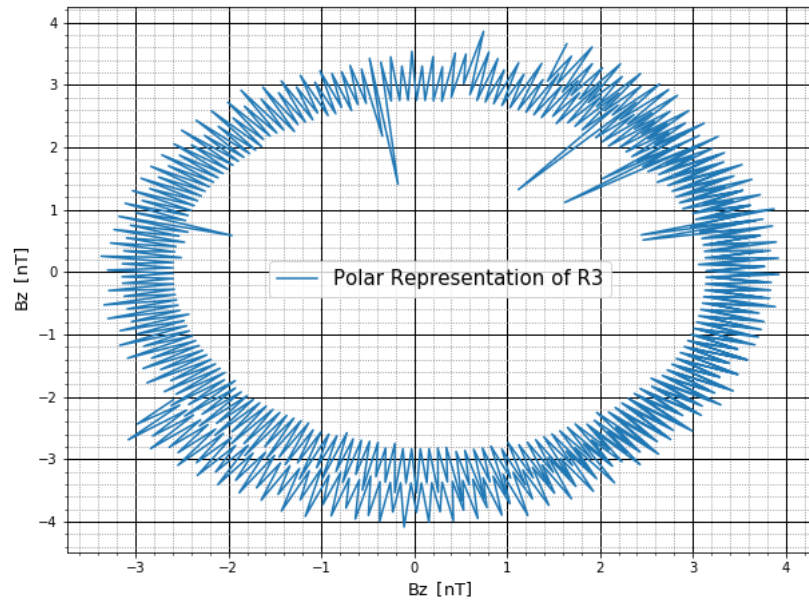


Figure 22: Polar Representation for one period of the signal coming from the R3 Conductor Loop.

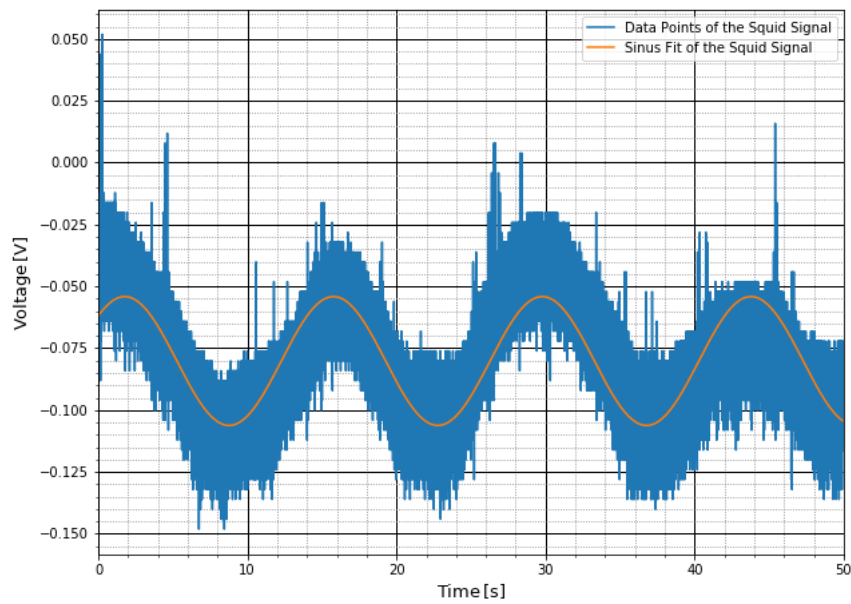


Figure 23: Plot 1 of the fourth conductor loop with resistor 4. The speed of the rotation here was 5. In orange is the sinus fit of the data point.

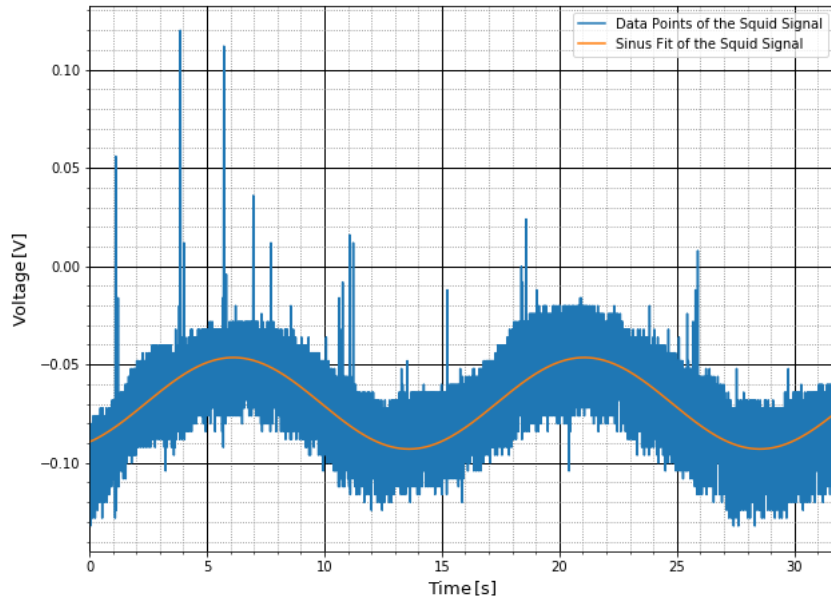


Figure 24: Plot 2 of the fourth conductor loop with resistor 4. The speed of the rotation here was 5. In orange is the sinus fit of the data point.

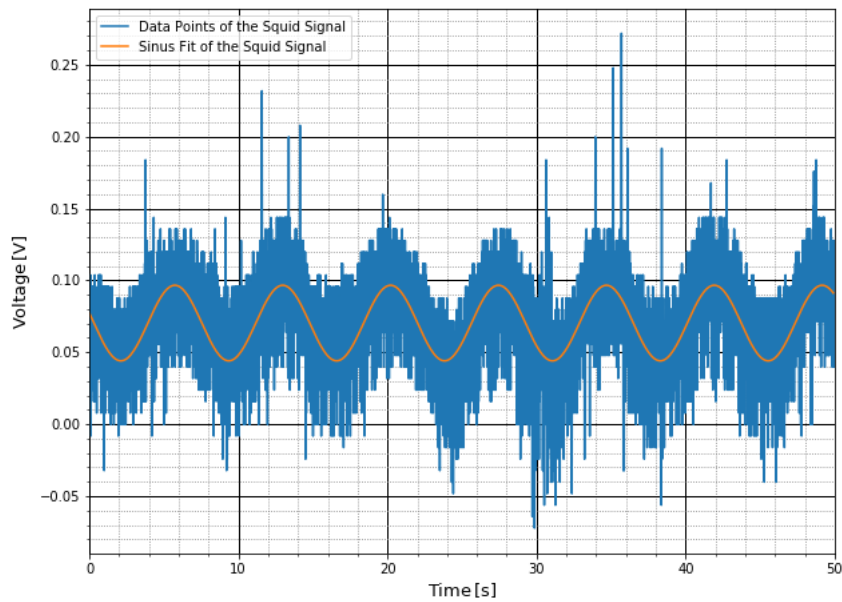


Figure 25: Plot 3 of the fourth conductor loop with resistor 4. The speed of the rotation here was 10. In orange is the sinus fit of the data point.

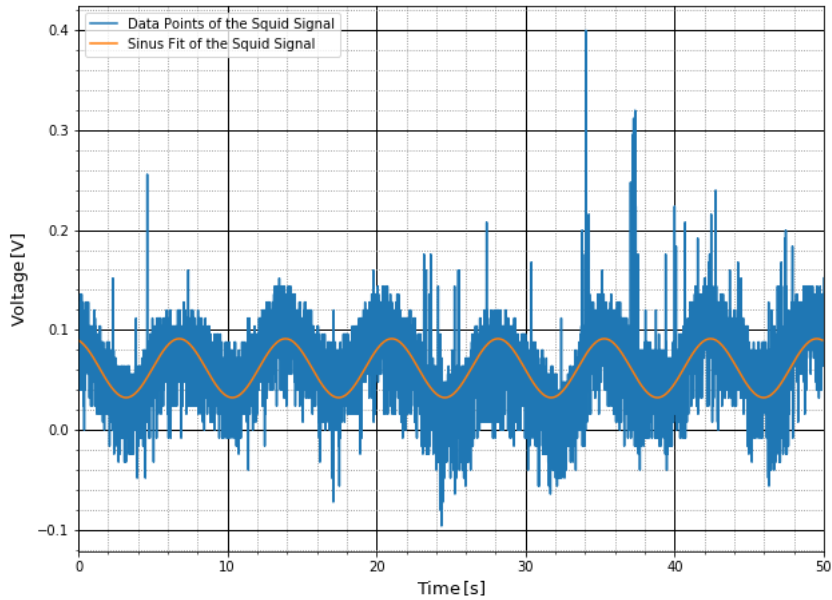


Figure 26: Plot 4 of the fourth conductor loop with resistor 4. The speed of the rotation here was 10. In orange is the sinus fit of the data point.

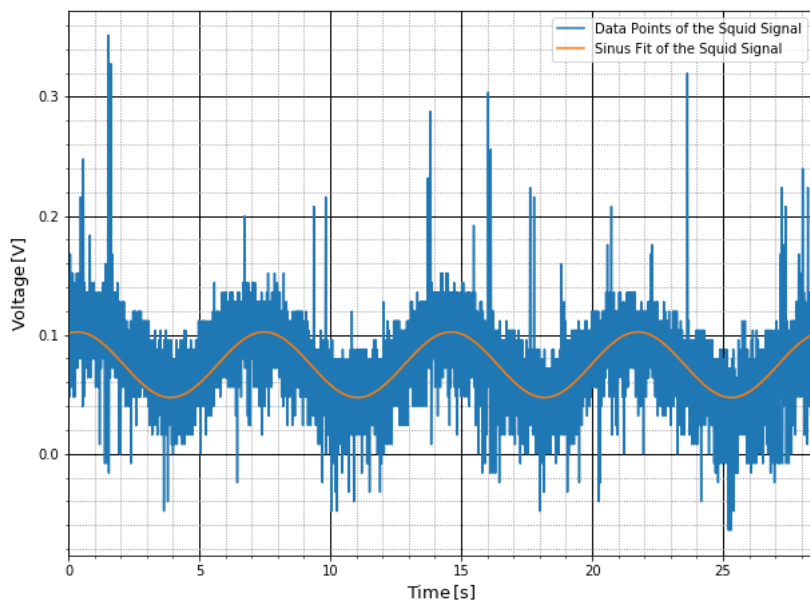


Figure 27: Plot 5 of the fourth conductor loop with resistor 4. The speed of the rotation here was 10. In orange is the sinus fit of the data point.

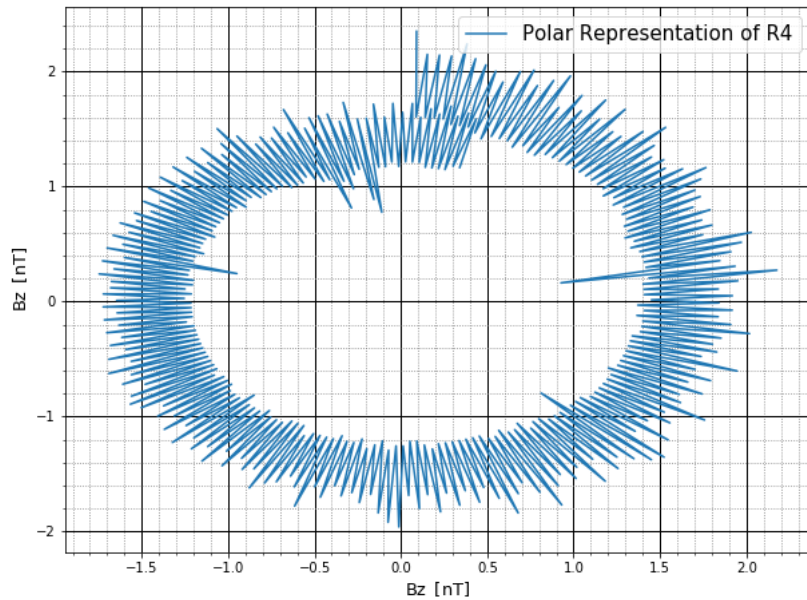


Figure 28: Polar Representation for one period of the signal coming from the R4 Conductor Loop.

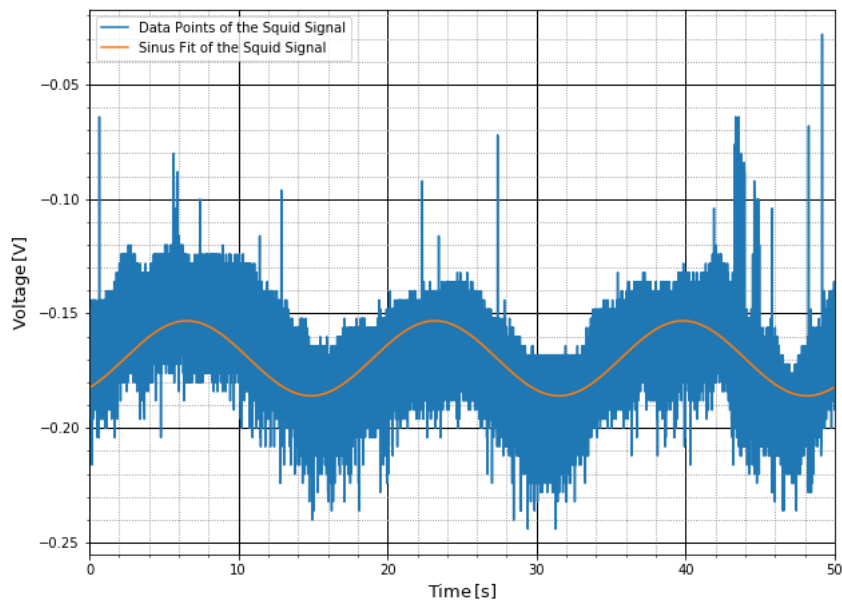


Figure 29: Plot 1 of the fifth conductor loop with resistor 5. The speed of the rotation here was 5. In orange is the sinus fit of the data point.

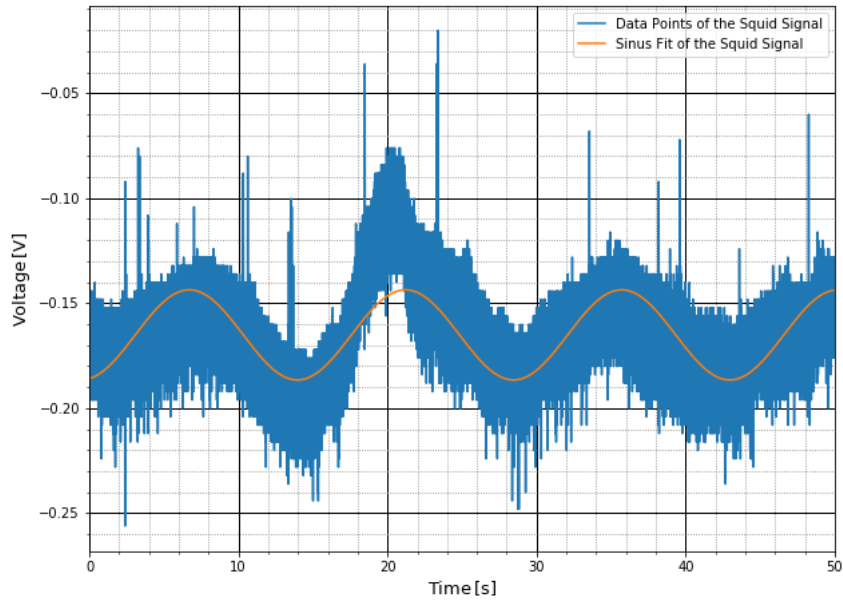


Figure 30: Plot 2 of the fifth conductor loop with resistor 5. The speed of the rotation here was 5. In orange is the sinus fit of the data point.

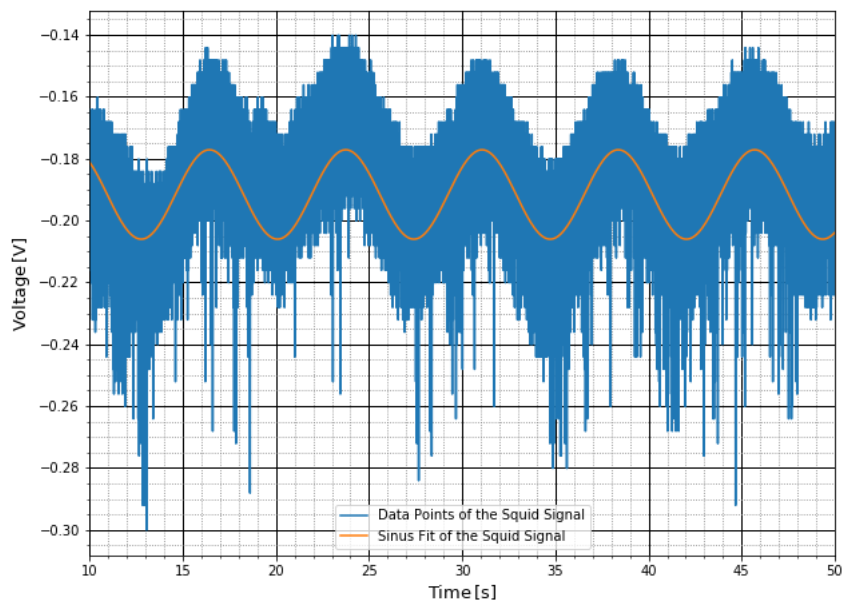


Figure 31: Plot 3 of the fifth conductor loop with resistor 5. The speed of the rotation here was 10. In orange is the sinus fit of the data point.

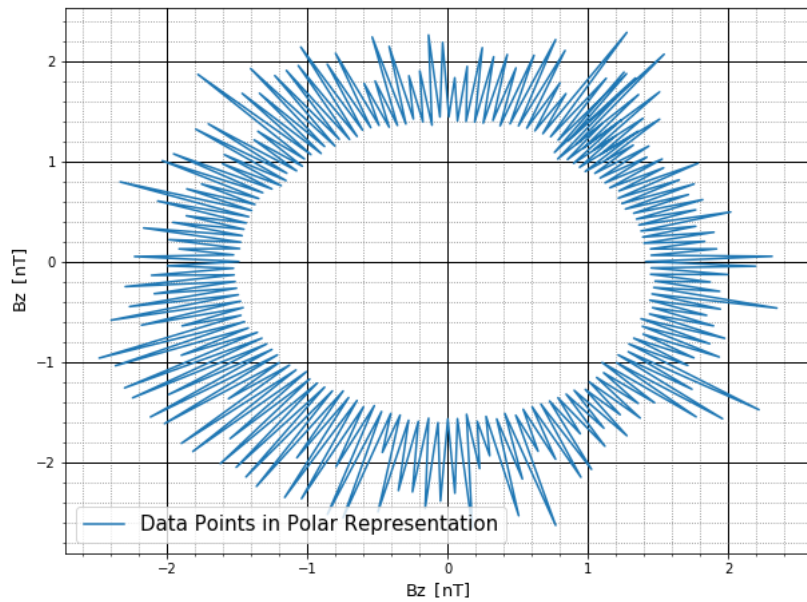


Figure 32: Polar Representation for one period of the signal coming from the R5 Conductor Loop.

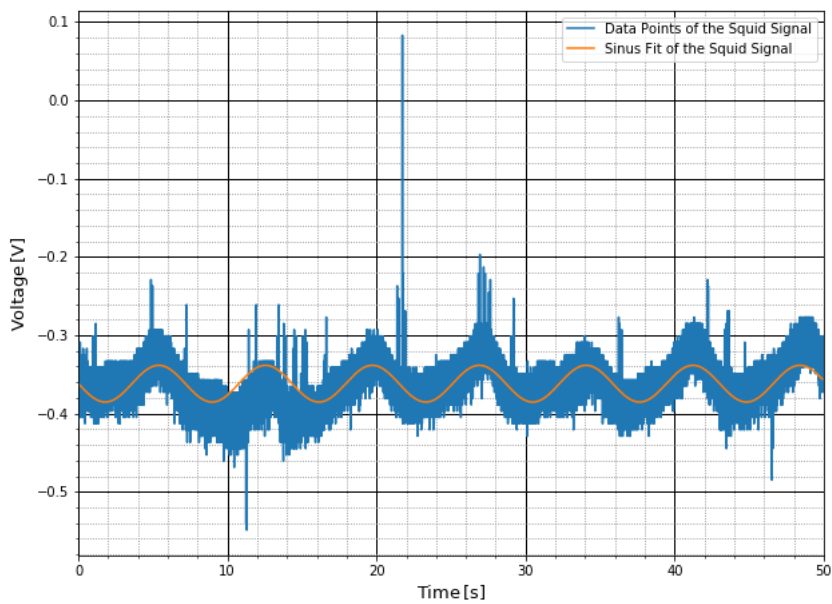


Figure 33: Plot of the SQUID signal with Iron chips as a sample.

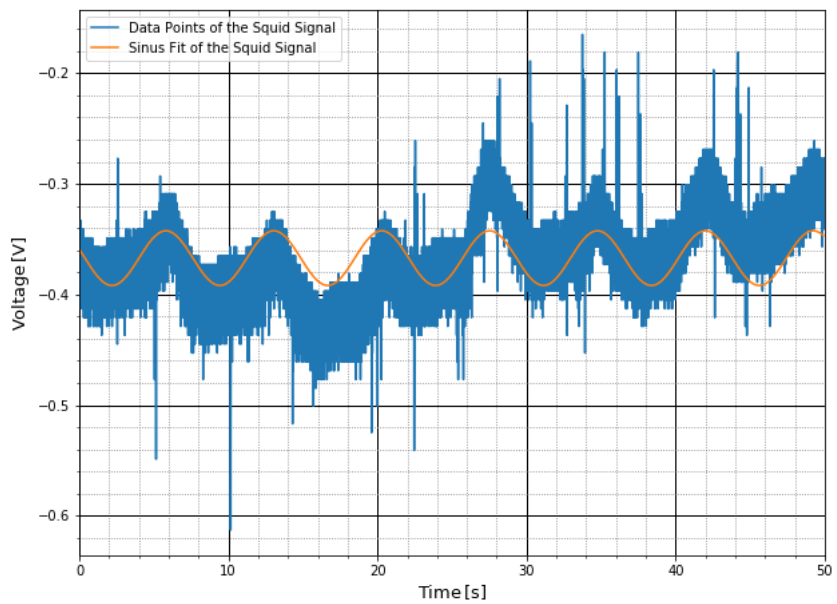


Figure 34: Plot of the SQUID signal with Iron chips as a sample.

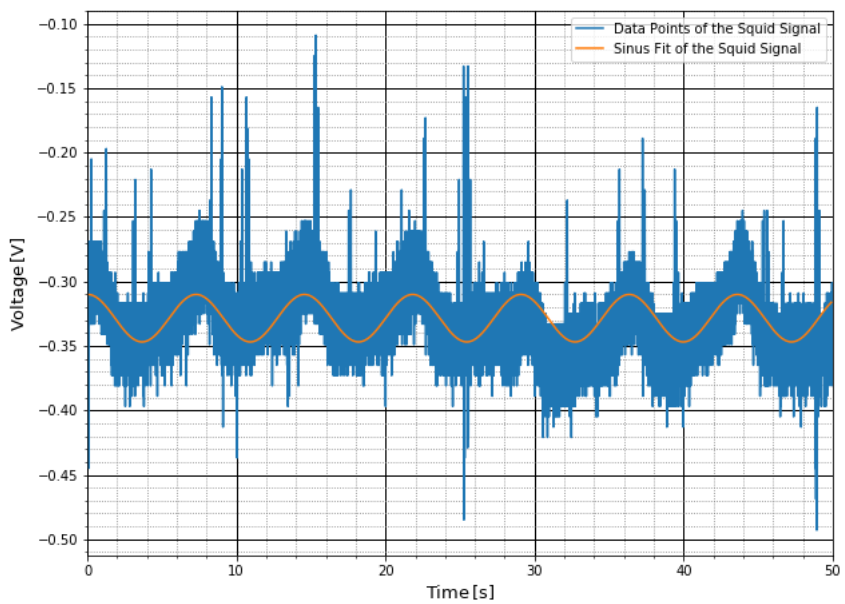


Figure 35: Plot of the SQUID signal with Iron chips as a sample.

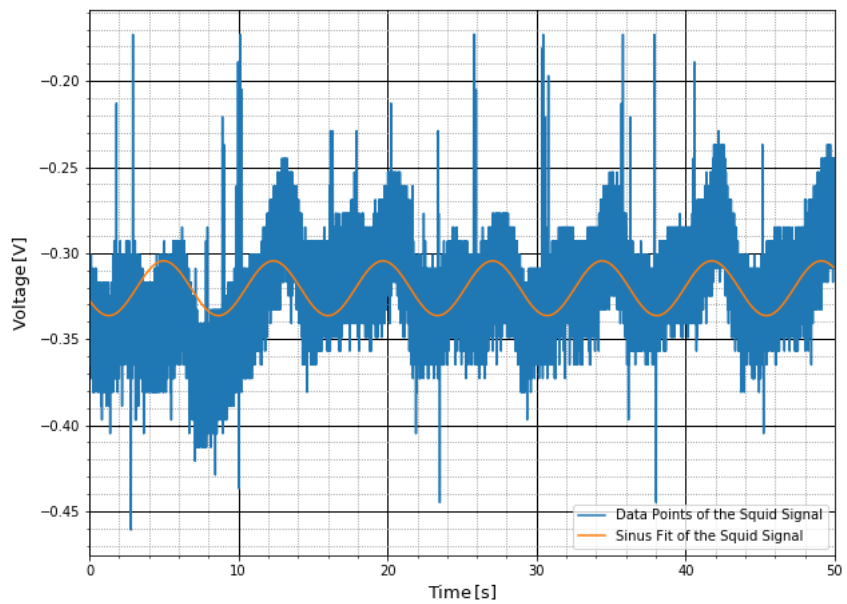


Figure 36: Plot of the SQUID signal with Iron chips as a sample.

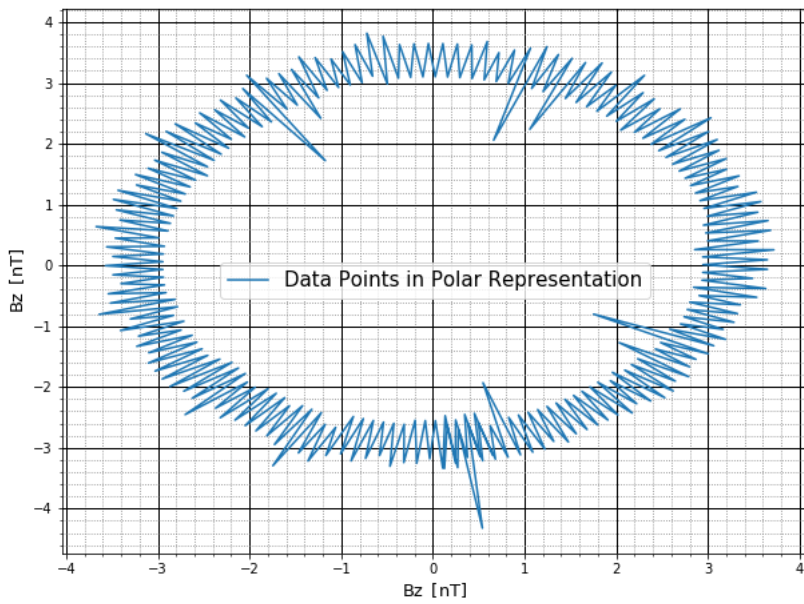


Figure 37: Polar Representation for one period of the signal coming from the iron chips.

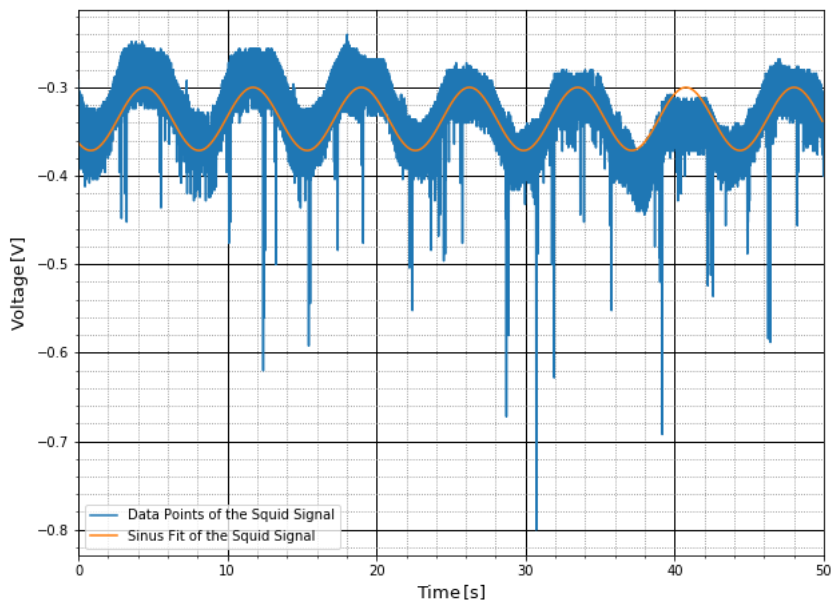


Figure 38: Plot of the SQUID signal with Gold Slide as a sample.

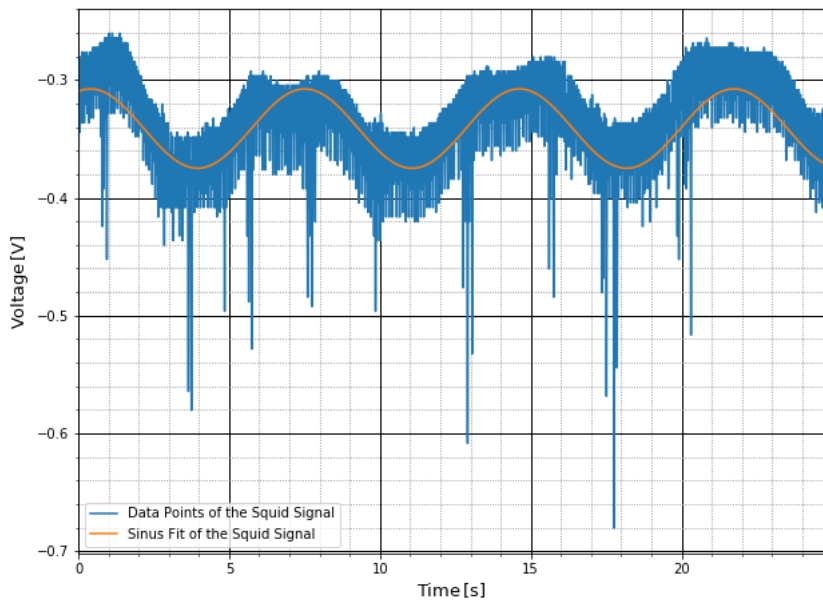


Figure 39: Plot of the SQUID signal with Gold Slide as a sample.

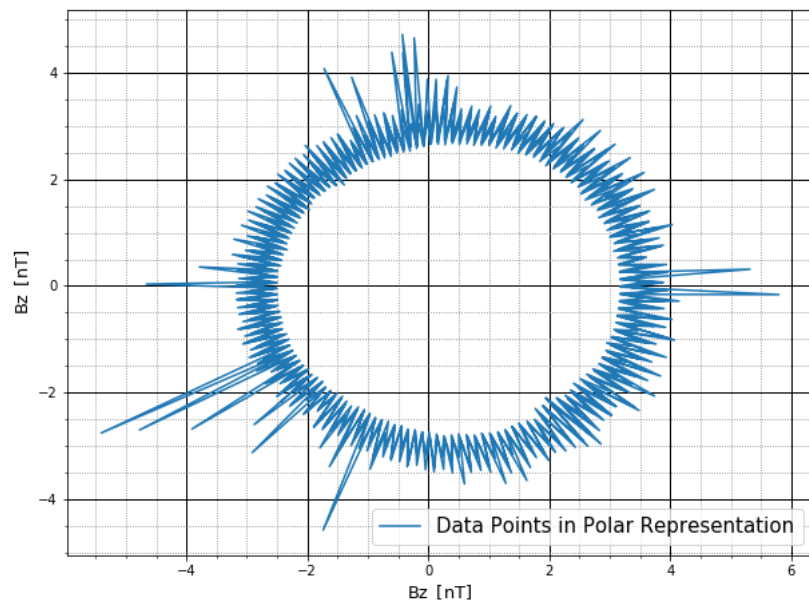


Figure 40: Polar Representation for one period of the signal coming from the gold slide.

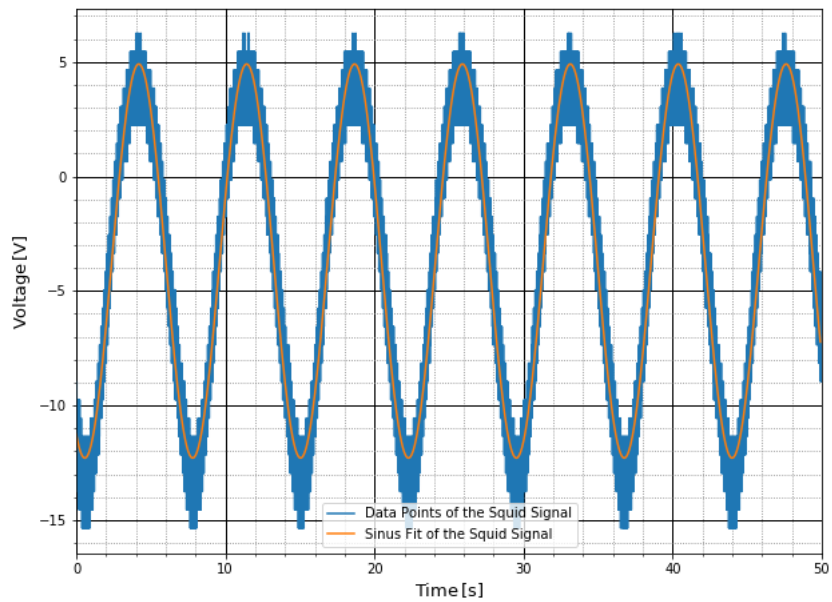


Figure 41: Plot of the SQUID signal with Magnet chips as a sample.

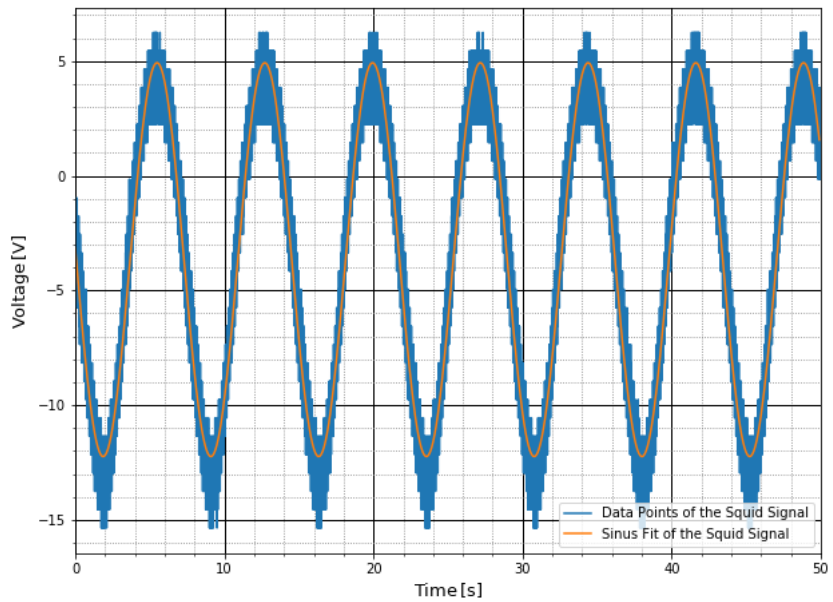


Figure 42: Plot of the SQUID signal with Magnet chips as a sample.

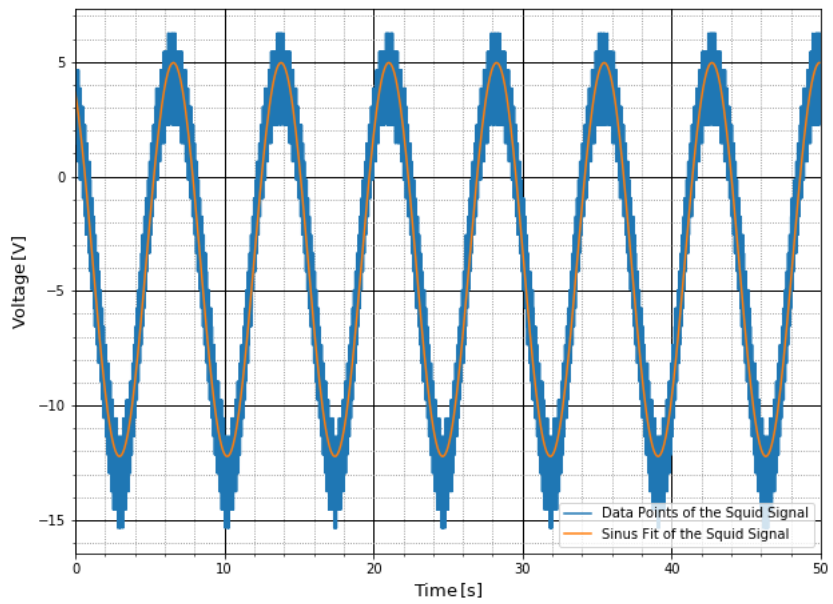


Figure 43: Plot of the SQUID signal with Magnet chips as a sample.

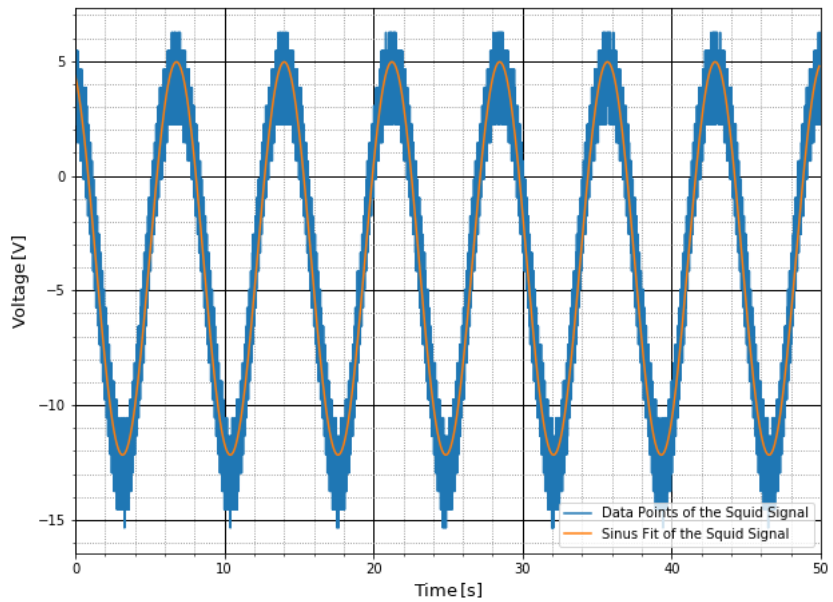


Figure 44: Plot of the SQUID signal with Magnet chips as a sample.

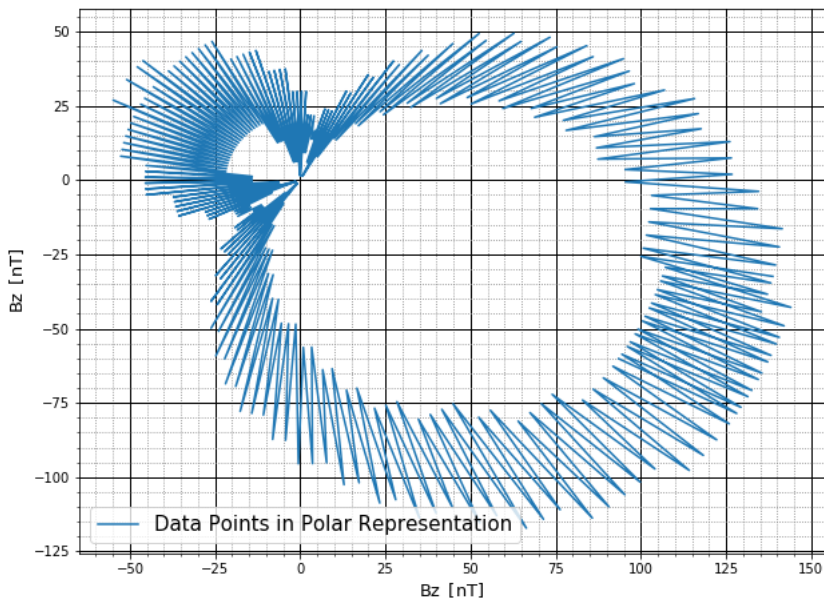


Figure 45: Polar Representation for one period of the signal coming from the magnet chips.

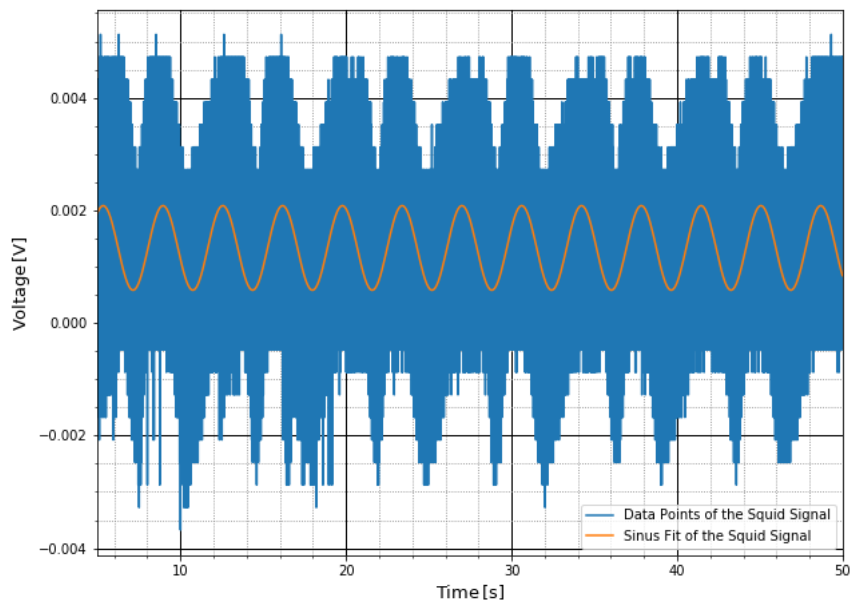


Figure 46: Plot of the SQUID signal with a stone as a sample.

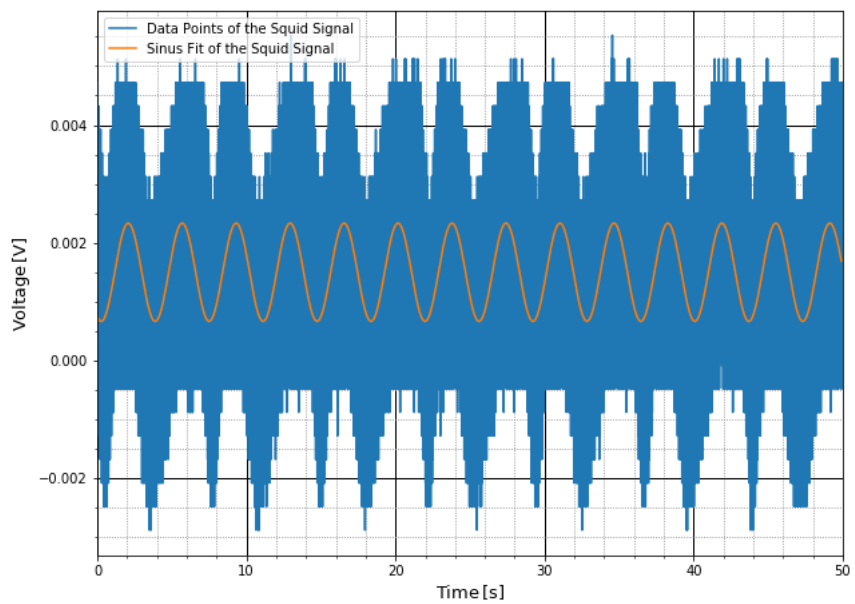


Figure 47: Plot of the SQUID signal with a stone as a sample.

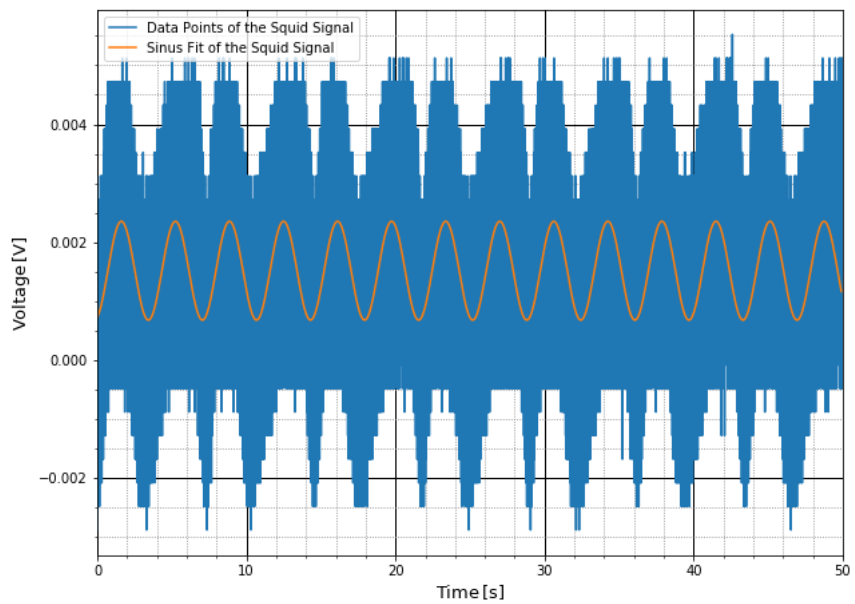


Figure 48: Plot of the SQUID signal with a stone as a sample.

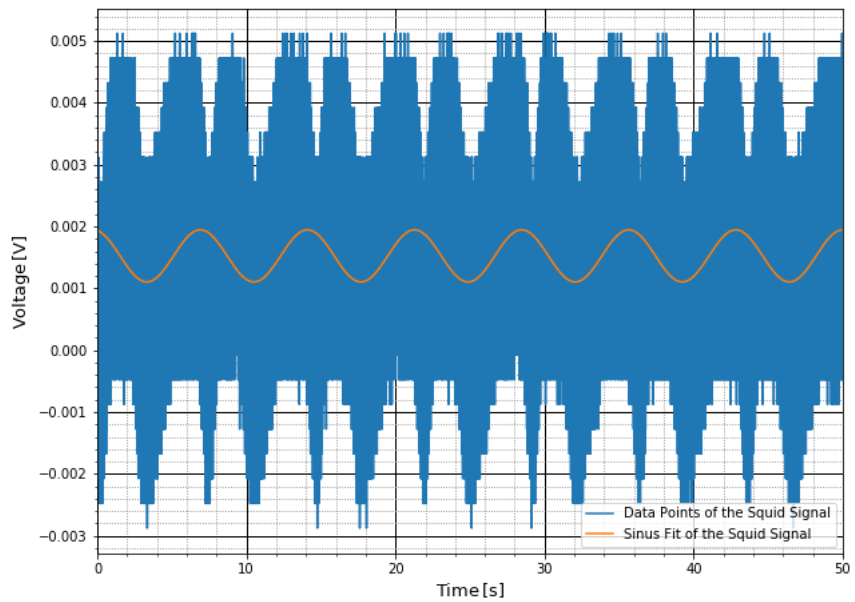


Figure 49: Plot of the SQUID signal with a Stone as a sample.

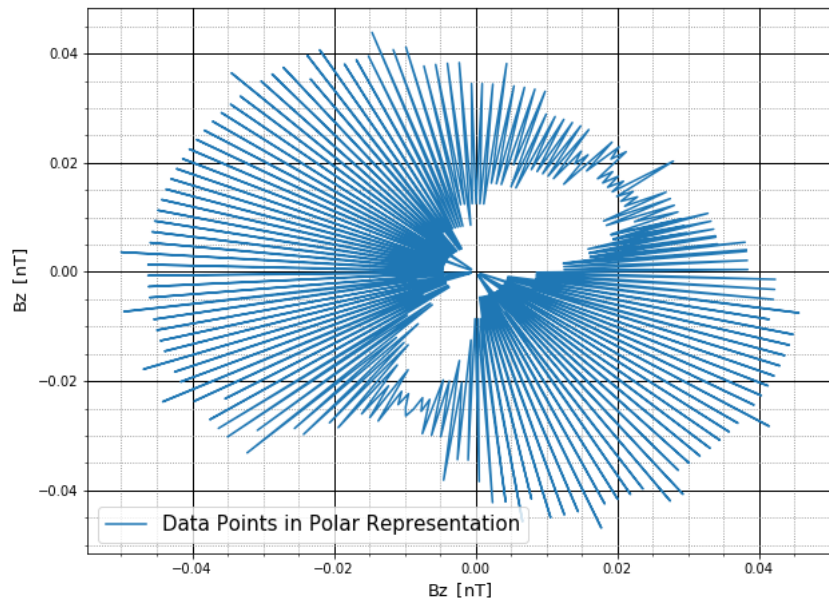


Figure 50: Polar Representation for one period of the signal coming from the stone.

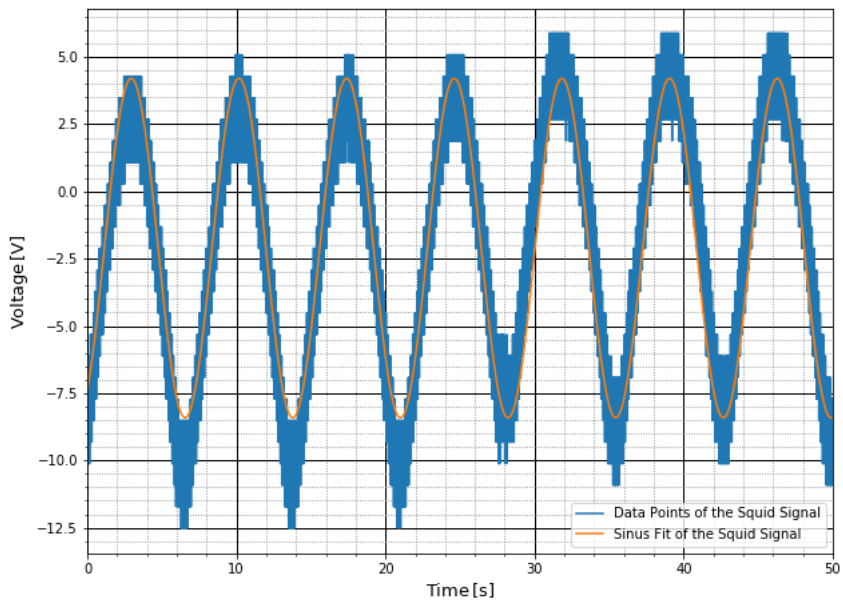


Figure 51: Plot of the SQUID signal with a magnet as a sample.

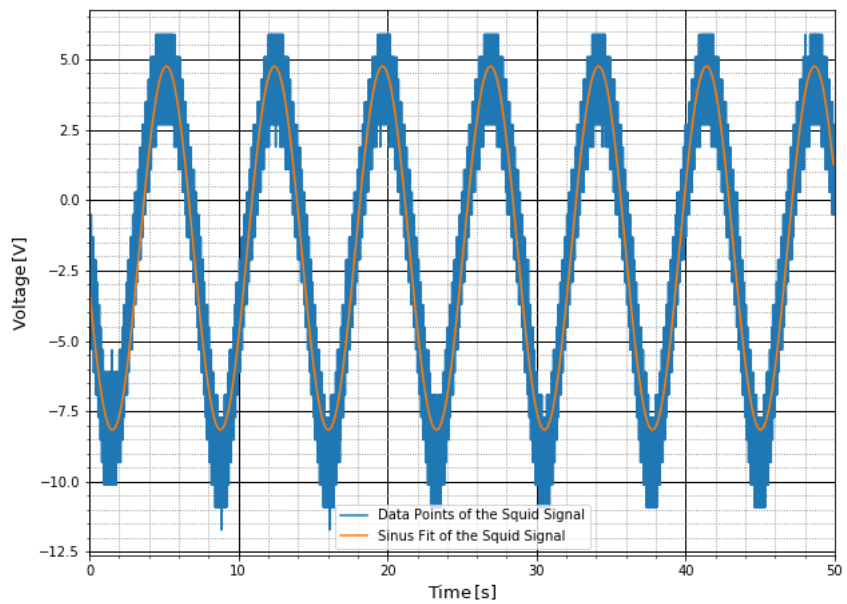


Figure 52: Plot of the SQUID signal with a magnet as a sample.

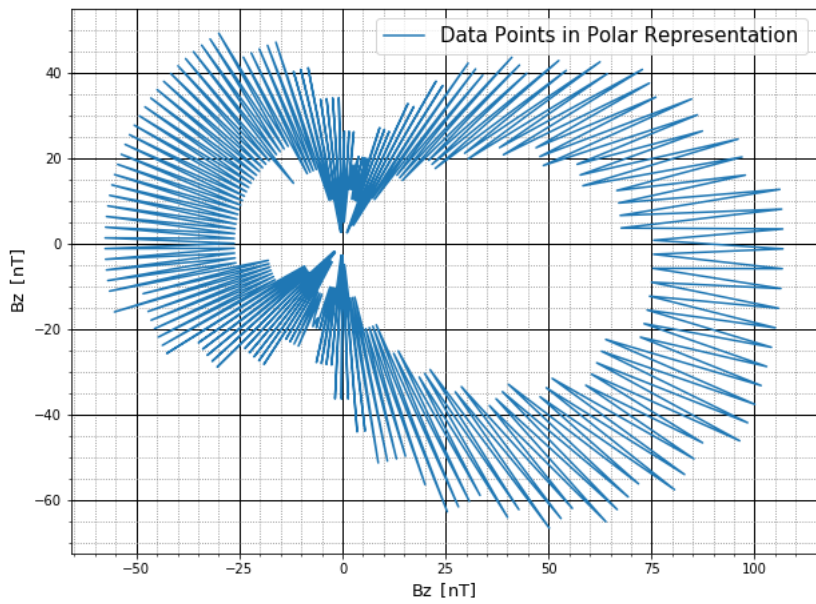


Figure 53: Polar Representation for one period of the signal coming from the magnet.